Title

Carbon Monoxide, a Retrograde Messenger Generated in Postsynaptic Mushroom Body Neurons, Evokes Noncanonical Dopamine Release

Journal

Journal of Neuroscience, 40(18)

ISSN

0270-6474

Authors

Ueno, Kohei
Morstein, Johannes
Ofusa, Kyoko
et al.

Publication Date

2020-04-29

DOI

10.1523/jneurosci.2378-19.2020

Peer reviewed

Cellular/Molecular

Carbon Monoxide, a Retrograde Messenger Generated in Postsynaptic Mushroom Body Neurons, Evokes Noncanonical Dopamine Release

Kohei Ueno,[1] Johannes Morstein,[2,3] Kyoko Ofusa,[1] Shintaro Naganos,[1] Ema Suzuki-Sawano,[1] Saika Minegishi,[4] Samir P. Rezgui,[5] Hiroaki Kitagishi,[4] Brian W. Michel,[5] Christopher J. Chang,[2] Junjiro Horiuchi,[1] and Minoru Saitoe[1]

[1]Tokyo Metropolitan Institute of Medical Science, Tokyo, 1568506, Japan, [2]Department of Chemistry and Department of Molecular and Cell Biology, University of California, Berkeley, California, 94720, [3]Department of Chemistry, New York University, New York, New York 10012, [4]Faculty of Science and Engineering, Doshisha University, Kyoto, 6100321, Japan, and [5]Department of Chemistry and Biochemistry, University of Denver, Denver, Colorado 80208

Dopaminergic neurons innervate extensive areas of the brain and release dopamine (DA) onto a wide range of target neurons. However, DA release is also precisely regulated. In *Drosophila melanogaster* brain explant preparations, DA is released specifically onto α3/α′3 compartments of mushroom body (MB) neurons that have been coincidentally activated by cholinergic and glutamatergic inputs. The mechanism for this precise release has been unclear. Here we found that coincidentally activated MB neurons generate carbon monoxide (CO), which functions as a retrograde signal evoking local DA release from presynaptic terminals. CO production depends on activity of heme oxygenase in postsynaptic MB neurons, and CO-evoked DA release requires Ca^{2+} efflux through ryanodine receptors in DA terminals. CO is only produced in MB areas receiving coincident activation, and removal of CO using scavengers blocks DA release. We propose that DA neurons use two distinct modes of transmission to produce global and local DA signaling.

Key words: **carbon monoxide; dopamine; *Drosophila*; retrograde messenger**

Significance Statement

Dopamine (DA) is needed for various higher brain functions, including memory formation. However, DA neurons form extensive synaptic connections, while memory formation requires highly specific and localized DA release. Here we identify a mechanism through which DA release from presynaptic terminals is controlled by postsynaptic activity. Postsynaptic neurons activated by cholinergic and glutamatergic inputs generate carbon monoxide, which acts as a retrograde messenger inducing presynaptic DA release. Released DA is required for memory-associated plasticity. Our work identifies a novel mechanism that restricts DA release to the specific postsynaptic sites that require DA during memory formation.

Introduction

Dopamine (DA) is required for various brain functions, including the regulation of global brain states, such as arousal and moods (Huang and Kandel, 1995; Molina-Luna et al., 2009; Yagishita et al., 2014). To perform these functions, individual DA neurons innervate extensive areas of the brain, and release DA onto a wide range of target neurons through a processes known as volume transmission (Agnati et al., 1995; Rice and Cragg, 2008; Matsuda et al., 2009). However, this extensive innervation is not suitable for precise, localized release of DA, and it has been unclear how widely innervating dopaminergic neurons can also direct DA release onto specific target neurons.

In *Drosophila*, olfactory associative memories are formed and stored in the mushroom bodies (MBs) where Kenyon cells, MB intrinsic neurons which are activated by different odors, form synaptic connections with various MB output neurons, which regulate approach and avoidance behaviors (Gerber et al., 2004;

Received Oct. 4, 2019; revised Feb. 12, 2020; accepted Mar. 19, 2020.

Author contributions: K.U. and M.S. designed research; K.U., K.O., S.N., and E.S.-S. performed research; S.M. and H.K. provided CO scavenger; J.M. and C.J.C. provided CO donor and CO probe; S.P.R. and B.W.M. measured the limit of detection of COP-1; K.U., J.H., and M.S. wrote the paper.

The authors declare no competing financial interests.

This work was supported by the Japanese Society for the Promotion of Science Grant JP17K07122 to K.U.; Takeda Science Foundation to K.U.; Grant-in-Aid for Scientific Research in Innovative Areas "Memory dynamism" JP25115006 to M.S.; and National Institutes of Health GM-79465, ES-28096, and ES-4705 to C.J.C. We thank Tomoyuki Miyashita, Motomi Matsuno, Taro Ueno, and Yukinori Hirano for helpful discussions.

Correspondence should be addressed to Kohei Ueno at ueno-kh@igakuken.or.jp or Minoru Saitoe at saito-mn@igakuken.or.jp.

https://doi.org/10.1523/JNEUROSCI.2378-19.2020

Aso et al., 2014). Dopaminergic neurons (DA neurons) modulate plasticity of synapses between Kenyon cells and MB output neurons (Claridge-Chang et al., 2009; Aso et al., 2010, 2012; Liu et al., 2012). However, while there are ~2000–2500 Kenyon cells that form thousands of synapses with MB output neurons, plasticity at these synapses is regulated by relatively few DA neurons (Mao and Davis, 2009). This indicates that canonical action potential-dependent release cannot fully explain DA release and plasticity. We recently determined that in *Drosophila,* synaptic vesicular (SV) exocytosis from DA terminals is restricted to MB neurons that have been activated by coincident inputs from odor-activated cholinergic pathways, and glutamatergic pathways, which convey somatosensory (pain) information (Ueno et al., 2017). Odor information is transmitted to the MBs by projection neurons from the antennal lobe (AL) (Marin et al., 2002; Wong et al., 2002), while somatosensory information is transmitted to the brain via ascending fibers of the ventral nerve cord (AFV). AL stimulation evokes Ca^{2+} responses in the MB by activating nAChRs, and AFV stimulation evokes Ca^{2+} responses in the MBs by activating N-Methyl-D-aspartate receptors (NMDARs) in the MBs (Ueno et al., 2013). Significantly, when the AL and AFV are stimulated simultaneously (AL + AFV) or the AL and NMDARs are stimulated simultaneously (AL + NMDA), plasticity occurs such that subsequent AL stimulations causes increased Ca^{2+} responses in the $\alpha3/\alpha'3$ compartments (Wang et al., 2008; Ueno et al., 2013). This plasticity is known as long-term enhancement (LTE) of MB responses and requires activation of D1 type DA receptors (D1Rs) in the MBs. Furthermore, while activation of D1Rs alone is sufficient to produce LTE, neither AL nor AFV stimulation alone is able to cause SV exocytosis from presynaptic DA terminals projecting onto the $\alpha3/\alpha'3$ compartments of the vertical MB lobes. Instead, exocytosis from DA terminals occurs only when postsynaptic Kenyon cells are activated by coincident AL + AFV or AL + NMDA stimulation. Strikingly, while MBs are bilateral structures and DA neurons project terminals onto both sides of MBs (Mao and Davis, 2009), SV exocytosis occurs specifically in MB areas that have been coincidently activated. Based on these results, we proposed that coincident inputs specify the location where DA is released, whereas DA induces plastic changes needed to encode associations. However, it has been unclear how activated Kenyon cells send a retrograde "demand" signal to presynaptic DA terminals to induce SV release.

In this study, we used a *Drosophila* dissected brain system to examine synaptic plasticity and DA release, and found that coincidentally activated postsynaptic Kenyon cells generate the retrograde messenger, carbon monoxide (CO). CO is generated by heme oxygenase (HO) in postsynaptic MB neurons, and induces DA release from presynaptic terminals by evoking Ca^{2+} release from internal stores via ryanodine receptors (RyRs). Thus, while individual DA neurons extensively innervate the MBs, on-demand SV exocytosis allows DA neurons to induce plasticity in specific target neurons.

Materials and Methods

Fly stock maintenance

All fly stocks were raised on standard cornmeal medium at 25 ± 2°C and 60 ± 10% humidity under a 12/12 h light-dark cycle. Flies were used for Experiments 1-3 d after eclosion. We used female flies for imaging and immunohistochemical studies, and used mixed populations of male and female flies for behavioral studies.

Table 1. Genotypes used in each experiment

Figure	Genotype
1A	*MB-LexA:GAD; LexAop-shi^{ts} as MB > shi^{ts}*
	MB-LexA:GAD
	LexAop-shi^{ts}
1B	*UAS-spH/MB-LexA:GAD;TH-GAL4/LexAop-shi^{ts}*
1C	*c747-GAL4/LexAop-spH;UAS-shi^{ts}/TH-LexAp65*
2A	*UAS-spH; TH-GAL4*
2B	*UAS-spH; TH-GAL4*
2C	*UAS-spH; TH-GAL4*
2D	*UAS-dicer/LexAop-spH;UAS-dHO-IR, MBsw/TH-LexAGAD*
3A	*MB-LexA:GAD, LexAop-G-CaMP2*
3B	*CS(w) as WT*
	Df(3R)Exel7309/+ as dHO$^{\Delta}$/+
3C	*UAS-dicer/MBLexA:GAD, LexAop-G-CaMP2;UAS-dHO-IR, MBsw/+*
3D	*UAS-dicer/+; MBsw, UAS-dHO-IR/Df(3R)Exel7309 as MBsw > UAS-dHO-KD*
	UAS-dicer/+; MBsw/Df(3R)Exel7309 as control
3E	*UAS-dicer/+; MBsw, UAS-dHO-IR/Df(3R)Exel7309*
4A	*UAS-DA1m; TH-GAL4*
4B	*UAS-DA1m; TH-GAL4*
5A	*UAS-spH; TH-GAL4*
5B	*UAS-spH; TH-GAL4*
5C	*UAS-spH; TH-GAL4*
5D	*UAS-spH; TH-GAL4*
5E	*UAS-spH; TH-GAL4*
6A	*MB-LexA:GAD, LexAop-R-GECO1*
6B	*MB-LexA:GAD, LexAop-R-GECO1*
6C	*MB-LexA:GAD, LexAop-R-GECO1/UAS-dicer; UAS-dHO-IR, MBsw*
7A	*MB-LexA:GAD, LexAop-R-GECO1/UAS-G-CaMP3; TH-GAL4*
7B	*MB-LexA:GAD, LexAop-R-GECO1/UAS-G-CaMP3; TH-GAL4*
7C	*UAS-G-CaMP3; TH-GAL4*
7D	*UAS-spH; TH-GAL4*
7E	*UAS-spH; TH-GAL4*
7F	*UAS-spH; TH-GAL4*
8A	*UAS-spH; TH-GAL4*
8B	*UAS-spH; TH-GAL4*
8C	*UAS-spH; TH-GAL4*
9A	*Mi{Trojan-GAL4.0}RyR[MI08146-TG4.0]/UAS-mCD8::GFP*
9B	*UAS-RyR RNAi, tubp-GAL80(ts)/LexAop-spH; TH-GAL4/TH-LexAp65*
	UAS-RyR RNAi, tubp-GAL80(ts)/LexAop-spH; TH-LexAp65/+
9C	*UAS-RyR RNAi, tubp-GAL80(ts)/LexAop-spH; TH-GAL4/TH-LexAp65*
	UAS-RyR RNAi, tubp-GAL80(ts)/LexAop-spH; TH-LexAp65/+
9D	*MB-LexA:GAD, LexAop-G-CaMP2/+; TH-GAL4 as control*
	UAS-RyR RNAi/ MB-LexA:GAD, LexAop-G-CaMP2; TH-GAL4 as TH >RyR-KD
9E	*UAS-RyR RNAi; TH-GAL4 as TH-GAL4>RyR-KD*
	UAS-RyR RNAi
	TH-GAL4
9F	*UAS-RyR RNAi; TH-GAL4 as TH-GAL4>RyR-KD*
	UAS-RyR RNAi

Transgenic and mutant lines

All transgenic and mutant lines used in this study are listed in Table 1. *UAS-G-CaMP3* (BDSC 32234, Bloomington Stock Center), *LexAop-G-CaMP2* (Ueno et al., 2013), and *LexAop-R-GECO1* lines were used for measuring Ca^{2+} responses as described previously (Ueno et al., 2013). *UAS-synapto-pHluorin* (*UAS-spH*) (Ng et al., 2002) and *LexAop-synapto-pHluorin* (*LexAop-spH*) lines were used for measuring vesicle release (Ueno et al., 2013). *MB-LexA::GAD* (Ueno et al., 2013) was used for the *LexA* MB driver, *c747* (Aso et al., 2009) was used as the *GAL4* MB driver, and *TH-GAL4* (Friggi-Grelin et al., 2003) and *TH-LexAp65* (Ueno et al., 2013) were used for *TH-DA* drivers. *UAS-shi^{ts}* (Kitamoto, 2001) and *pJFRC104-13XLexAop2-IVS-Syn21-Shibire-ts1-p10* (*LexAop-shi^{ts}*) (Pfeiffer et al., 2012) lines were used for inhibition of synaptic transmission. *MB247-Switch* (*MBsw*) was used to express a *UAS* transgene in the MBs on RU486 (RU^{+}) feeding for 3–5 d (Mao et al., 2004). *UAS-dHO IR* was used to knockdown of *dHO* expression (Cui et al., 2008). *dHO$^{\Delta}$* is a deficiency line *Df(3R)Exel7309* (BDSC 7960), lacking

65 Kbp, including *dHO* (Flybase; http://flybase.org) in the third chromosome. *UAS-DA1m* was used for detecting extracellular DA amounts (Sun et al., 2018). *P{KK101716}VIE-260B* (VDRC ID 109631, Vienna Drosophila Resource Center) (*UAS-RyR RNAi*) was used to knock down *RyR*. *Mi{Trojan-GAL4.0}RyR[MI08146-TG4.0]* (BDSC 67480) carries a *GAL4* sequence between exons 18 and 19 of *RyR* and was used to monitor *RyR* gene expression.

Isolated whole-brain preparations

Brains were prepared for imaging as previously described (Ueno et al., 2013). Briefly, brains were dissected in ice cold 0 mM Ca^{2+} HL3 medium (in mM as follows: 70 NaCl, 115 sucrose 115; 5 KCl, 20 $MgCl_2$, 10 $NaHCO_3$, 5 Trehalose, 5 HEPES, pH 7.3, 359 mOsm) (Stewart et al., 1994), and placed in a recording chamber filled with normal, room temperature HL3 medium (the same recipe as above, containing 1.8 mM $CaCl_2$). To deliver hemoCD through the blood-brain barrier, brains were treated with papain (10 U/ml) for 15 min at room temperature, and washed several times with 0 mM Ca^{2+} HL3 medium before use (Gu and O'Dowd, 2007; Ueno et al., 2017).

Imaging analysis

Imaging analysis was performed in HL3 solution as described previously (Ueno et al., 2013, 2017). Briefly, fluorescent images were captured at 15 Hz using a confocal microscope system (A1R, Nikon) with a 20× water-immersion lens (numerical aperture 0.5; Nikon). We obtained F_0 by averaging the 5 sequential frames before stimulus onset and calculated $\Delta F/F_0$. To evaluate stimulation-induced fluorescent changes of spH, $\Delta F/F_0$ calculated in the absence of stimulation or pharmacological agents was subtracted from stimulus or drug-induced $\Delta F/F_0$. To quantitatively evaluate spH fluorescent changes, the average values of fluorescent changes at indicated time points during and after stimulation were statistically compared.

The AL was stimulated (30 pulses, 100 Hz, 1.0 ms pulse duration) using glass micro-electrodes. For NMDA stimulation, 200 μM NMDA, diluted in HL3 containing 4 mM Mg^{2+} (Miyashita et al., 2012), was bath-applied to the recording chamber. Thus, all NMDARs on the MB were simultaneously activated.

For application of CO-saturated HL3, CO or control N_2 gas was dissolved in HL3 saline by bubbling. CO or N_2 saturated solutions were immediately placed in glass pipettes and puffed onto the MB lobes for 1 min (pressure = 6 psi) using a Picospritzer III system (Parker Hannifin). While we first used thin tip micropipettes, ~5 μm diameter (see Fig. 5*A*), we also used larger tip micropipettes, ~15 μm (see Fig. 9*C*), to avoid clogging.

Behaviors

Olfactory aversive memory. The procedure for measuring olfactory memory has been previously described (Tully and Quinn, 1985; Tamura et al., 2003). Briefly, two mildly aversive odors (3-octanol [OCT]) or 4-methylcyclohexanol [MCH]) were sequentially delivered to ~100 flies for 1 min with a 45 s interval between each odor presentation. When flies were exposed to the first, CS^+ odor (either OCT or MCH), they were also subjected to 1.5 s pulses of 60 V DC electric shocks every 5 s. To test olfactory memory, flies were placed at the choice point of a T-maze where they were allowed to choose either the CS^+ or CS^- odor for 1.5 min. Memory was calculated as a performance index (PI), such that a 50:50 distribution (no memory) yielded a performance index of zero and a 0:100 distribution away from the CS^+ yielded a performance index of 100.

Odor and shock avoidance. Peripheral control experiments including odor and shock reactivity assays were performed as previously described (Tully and Quinn, 1985) to measure sensitivity to odors and electrical shocks. Approximately 100 flies were placed at the choice point of a T-maze where they had to choose between an odor (OCT or MCH) and mineral oil or between electrical shocks and nonshocked conditions. A performance index was calculated as described above.

Identification of dHO localization

To detect dHO protein in fly brains, WT, w(CS) (Dura et al., 1993), and dHO^{Δ} flies were dissected and fixed in 4% PFA for 20 min at 4°C. Brains were incubated in PBS with 5% FBS and 0.1% Triton-X for 30 min at 4°C, and then in primary antibodies, 1:50 anti-HO (Cui et al., 2008) and 1:20 anti-Fas2 (1D4, Developmental Studies Hybridoma Bank) for 3 d at 4°C. After washing, brains were incubated with secondary antibodies, Alexa488-conjugated donkey anti-rat antibody (1:200) (Invitrogen) and Alexa555-conjugated donkey anti-mouse antibody (1:200) (Invitrogen) for 2 d at 4°C. Images were captured using an A1R confocal microscope (Nikon).

Identification of RyR positive neurons (Trojan)

For *Mi{Trojan-GAL4.0}RyR[MI08146-TG4.0]/UAS-mCD8::GFP* imaging, heads were dissected and incubated in 4% PFA for 30 min at 4°C. Brains were incubated with primary antibodies, anti-GFP (1:400) (ab13970, Abcam) and anti-TH (#22941, Immunostar) in PBS with 10% ImmunoBlock (DS Pharma Biomedical) and 0.1% Triton-X overnight at 4°C. After washing, brains were incubated with secondary antibodies, Alexa488-conjugated donkey anti-chick antibody (1:400) (Jackson ImmunoResearch Laboratories) and Alexa555-conjugated donkey anti-mouse antibody (1:400) (Invitrogen) overnight at 4°C. Images were captured using an A1R confocal microscope (Nikon).

Chemicals and treatments

RU486 (mifepristone), NMDA, L-NAME, 1-octanol, 2-arachidonil glycerol, arachidonic acid, and chromium mesoporphyrin (CrMP) were purchased from Sigma Millipore. Thapsigargin and tetrodotoxin (TTX) were purchased from Wako Pure Chemical Industries. Dantrolene was purchased from Alomone Labs. BAPTA-AM and EGTA were purchased from Dojindo Lab. Papain was purchased from Worthington Biochemical. RU486 was dissolved in ethanol, butaclamol was dissolved in dimethyl sulfoxide DMSO), L-NAME was dissolved in water, and CrMP was dissolved in 0.5% 2-aminoethanol and 2 mM HCl. Oxy-hemoCD was reduced in sodium dithionite, purified using a HiTrap Desalting column (GE Healthcare) and eluted in PBS. The concentration of purified oxy-hemoCD was estimated by absorbance at 422 nm (Kitagishi et al., 2010). CO Probe 1 (COP-1) and CO-releasing molecule-3 (CORM-3) were prepared according to previous publications (Clark et al., 2003; Michel et al., 2012). Both reagents were stored at −20°C and dissolved in DMSO before use. For RU486 treatment, dissolved RU486 was mixed in fly food. Flies were fed RU486 for 5 d before brain preparation. Other chemicals were treated as described in the main text and figure legends.

Statistics

Statistical analyses were performed using Prism software (GraphPad Software). Trace graphs indicate mean values ± SEM. Boxes indicate 25th, 50th, and 75th centiles, whiskers indicate minimum and maximum and black dots indicate individual raw data. Student's *t* tests or Mann Whitney tests were used to evaluate the statistical significance between pairs of datasets. For multiple comparisons, one-way or two-way ANOVA followed by Bonferroni *post hoc* analyses was used. In all figures, NS indicates $p > 0.05$, * indicates $p < 0.05$, and ** indicates $p < 0.01$.

Results

CO synthesis in MB neurons is required for DA release on coincident stimulation

Previously, we used an *ex vivo* dissected brain system to examine SV exocytosis from DA terminals projecting onto the $\alpha 3/\alpha' 3$ compartments of the vertical MB lobes. We measured SV exocytosis from DA terminals using a vesicular exocytosis sensor, synapto-pHluorin (spH) (Miesenbock et al., 1998), expressed in dopaminergic neurons using a TH driver, and found that release occurred only on coincident activation of postsynaptic MB neurons by cholinergic inputs from the ALs and glutamatergic inputs from the AFV (Ueno et al., 2017).

If postsynaptic MB activity evokes SV exocytosis from presynaptic DA terminals, vesicular output from MB neurons may be needed to activate DA neurons that loop back to the MBs, as has

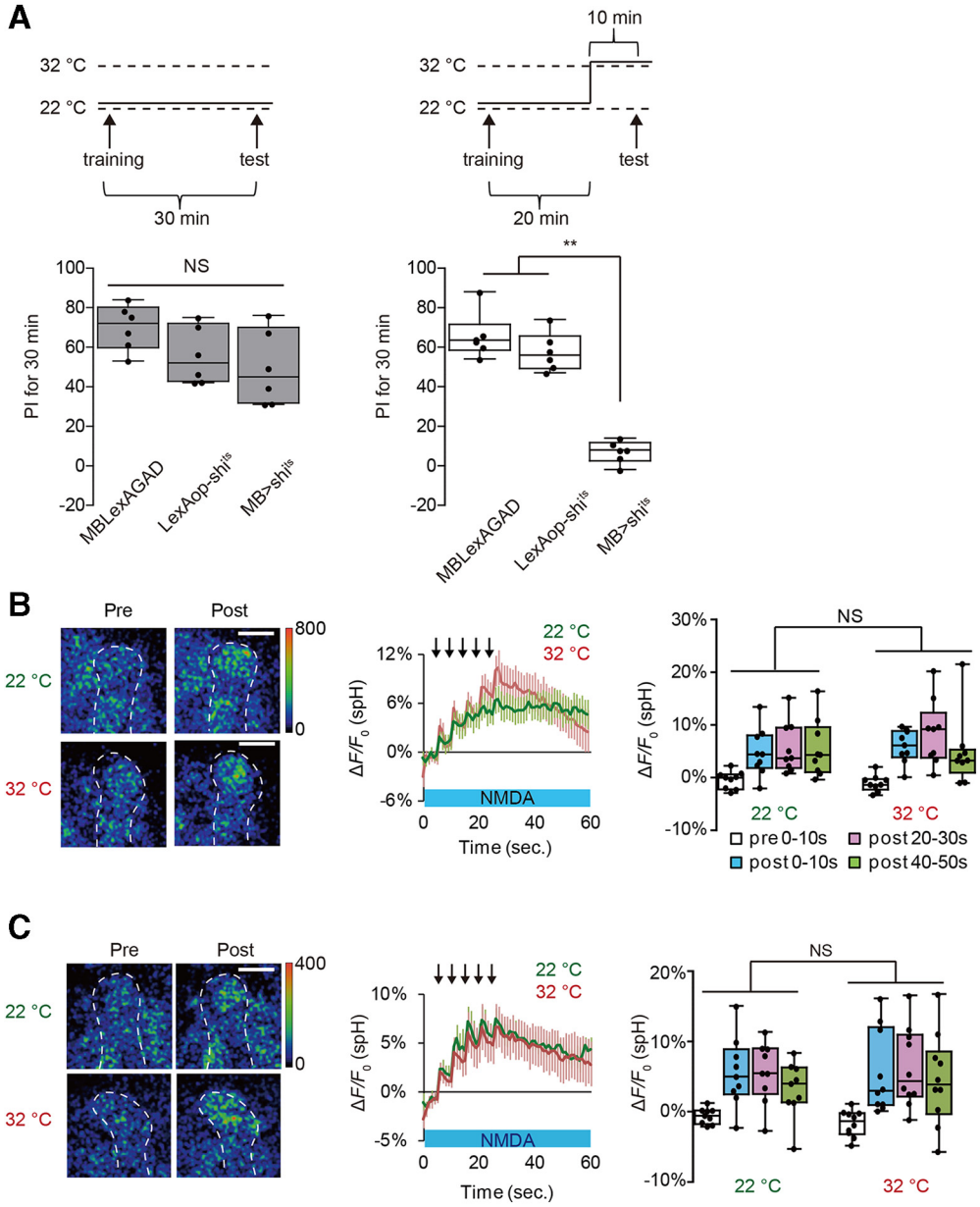

Figure 1. MB output is not required for DA release on coincident MB stimulation. ***A***, Inhibiting MB output impairs recall of olfactory memory. One-way ANOVA and Bonferroni *post hoc* tests indicate significant impairment in memory recall in *MB > shi^{ts}* flies at a restrictive temperature (32°C) ($F_{(2,15)} = 71.05$, $p < 0.001$) but not at a permissive temperature (22°C) ($F_{(2,15)} = 2.854$, $p = 0.09$). $^{**}p < 0.01$. Not significant ($p > 0.05$). $N = 6$ for all data. ***B***, ***C***, Blocking SV exocytosis from the MBs does not affect DA release. spH fluorescence was measured at TH-DA terminals innervating the $\alpha3/\alpha'3$ compartments of the MB vertical lobes in *MB-LexA>LexAop-shi^{ts}* (***B***) and *c747-GAL4>UAS-shi^{ts}* brains (***C***). Left, Typical pseudocolor images 5 s before and 30 s after coincident AL + NMDA activation. Middle, Time course of fluorescent changes. Arrows represent AL stimulation. Right, Summary graphs. Two-way ANOVA indicates no significant differences in spH fluorescence between restrictive (32°C) and permissive (22°C) temperatures in both *MB-LexA>LexAop-shi^{ts}* ($F_{(3,64)} = 2.854$, $p = 0.5716$, $N = 9$ for all data) and *c747-GAL4>UAS-shi^{ts}* ($F_{(3,68)} = 2.854$, $p = 0.01$, $N = 9$ for 22°C, $N = 10$ for 32°C). Scale bars, 20 μm.

been previously suggested (Ichinose et al., 2015; Cervantes-Sandoval et al., 2017; Takemura et al., 2017; Horiuchi, 2019). To test this possibility, we inhibited synaptic transmission from MB neurons by expressing temperature-sensitive *shi^{ts}* from a pan-MB driver, *MB-LexA*. We confirmed that MB synaptic output is blocked at restrictive temperature in *MB-LexA>LexAop-shi^{ts}* flies by demonstrating that memory recall, which requires MB output (Dubnau et al., 2001; McGuire et al., 2001), is defective in these flies (Fig. 1*A*). Interestingly, SV exocytosis from TH-DA terminals occurs normally at restrictive temperature in these flies on coincident AL + NMDA stimulation (Fig. 1*B*), suggesting that, while looping activity may be necessary for memory, it is not required for DA release. SV exocytosis from TH-DA terminals also occurred normally when *shi^{ts}* was expressed using a different MB driver (*c747-GAL4>UAS-shi^{ts}*) (Fig. 1*C*), although memory recall is also disrupted at restrictive temperature in this line (Dubnau et al., 2001). Also, 1 mM 1-octanol, a blocker of gap junctional communication (Rorig et al., 1996; Goncharenko et al., 2014), did not inhibit SV exocytosis in TH-DA terminals (Fig. 2*A*). These results suggest that output from chemical and electrical synapses is not required for postsynaptic MB neurons to induce presynaptic DA release from DA neurons.

We next examined whether a retrograde messenger, such as nitric oxide (NO), may be released from MB neurons to regulate presynaptic DA release. However, 100 μM L-NAME (Nω-L-nitro

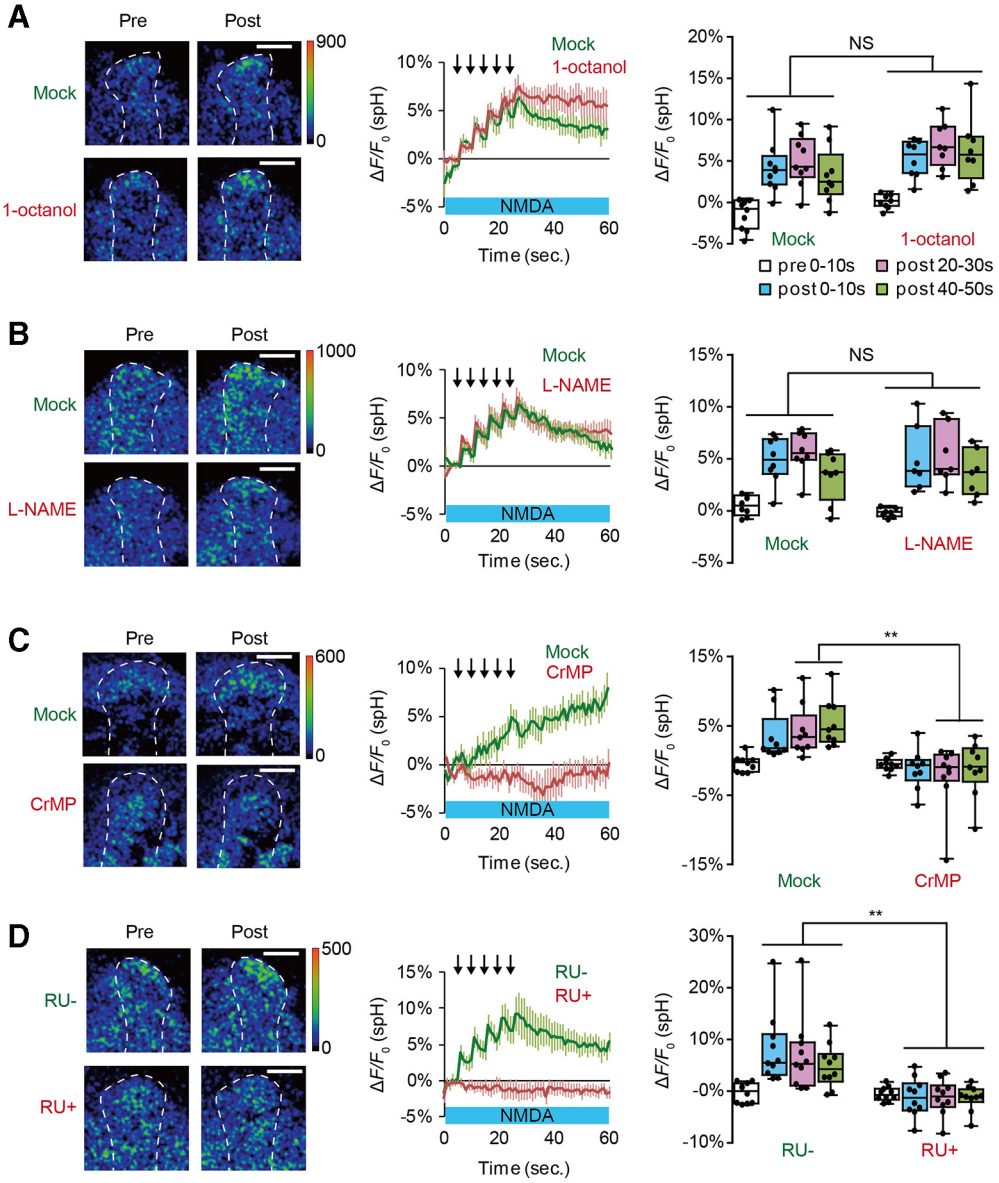

Figure 2. Inhibiting HO activity in the MBs blocks SV exocytosis from presynaptic DA terminals. ***A***, The gap junction inhibitor, 1-octanol, does not affect DA release. Two-way ANOVA indicates no significant differences in spH fluorescence between mock and 1-octanol conditions ($F_{(3,60)} = 0.3567$, $p = 0.785$). $N = 9$ for mock and $N = 8$ for 1 mM 1-octanol. ***B***, The NOS inhibitor, L-NAME, does not affect SV exocytosis from TH-DA terminals. Two-way ANOVA indicates no significant differences in spH fluorescence due to drug treatment ($F_{(3,52)} = 0.133$, $p = 0.940$). $N = 8$ for mock and $N = 7$ for 100 μM L-NAME. ***C***, The HO inhibitor, CrMP, prevents DA release. Two-way ANOVA indicates significant differences in spH fluorescence due to drug treatment ($F_{(3,64)} = 3.268$, $p = 0.0268$, $N = 9$ for mock and $N = 10$ for 10 μM CrMP). $^{**}p < 0.01$; Bonferroni *post hoc* tests. ***D***, *dHO* knockdown in the MBs prevents DA release. Two-way ANOVA indicates significant differences in spH fluorescence due to RU treatment ($F_{(3,72)} = 4.265$, $p = 0.0079$, $N = 10$ for all data). $^{**}p < 0.01$ (Bonferroni *post hoc* tests).

arginine methyl ester), a NO synthetase blocker (Boultadakis and Pitsikas, 2010), had no effect on AL + NMDA stimulation-induced SV exocytosis from TH-DA terminals (Fig. 2*B*).

Olfactory memory is disrupted by mutations in *nemy*, a gene that encodes a *Drosophila* homolog of cytochrome B561 (CytB561) (Iliadi et al., 2008), which is involved in metabolism of CO (Sugimura et al., 1980; Cypionka and Meyer, 1983; Jacobitz and Meyer, 1989), a diffusible gas similar to NO, that has also been proposed to act as a retrograde messenger during synaptic plasticity (Alkadhi et al., 2001; Shibuki et al., 2001). Thus, we examined whether CO may be required for DA release. CO is synthesized by HO, and we found that exocytosis from TH-DA terminals on coincident activation of MB neurons is abolished on application of CrMP, an HO blocker (Vreman et al., 1993) (Fig. 2*C*). LTE was also significantly inhibited by CrMP (Fig. 3*A*), demonstrating the importance of HO in plasticity. To verify that the *Drosophila* homolog of HO (*dHO*) (Cui et al., 2008) is present in the MBs, we used anti-dHO antibodies and found strong expression in the MBs and in insulin-producing cells (Fig. 3*B*). We next inhibited *dHO* expression in the MBs using *MBsw>UAS-dHO-IR* flies, which express a *dHO-RNAi* construct from an RU486-inducible *MB247-switch* (*MBsw*) driver (Mao et al., 2004). We found that both SV exocytosis from TH-DA terminals (Fig. 2*D*) as well as LTE (Fig. 3*C*) were impaired when these flies were fed RU486. Furthermore, acute knockdown of *dHO* in the MBs in *MBsw>UAS-dHO-IR* flies disrupted olfactory memory (Fig. 3*D*) without affecting task-related responses (Fig. 3*E*).

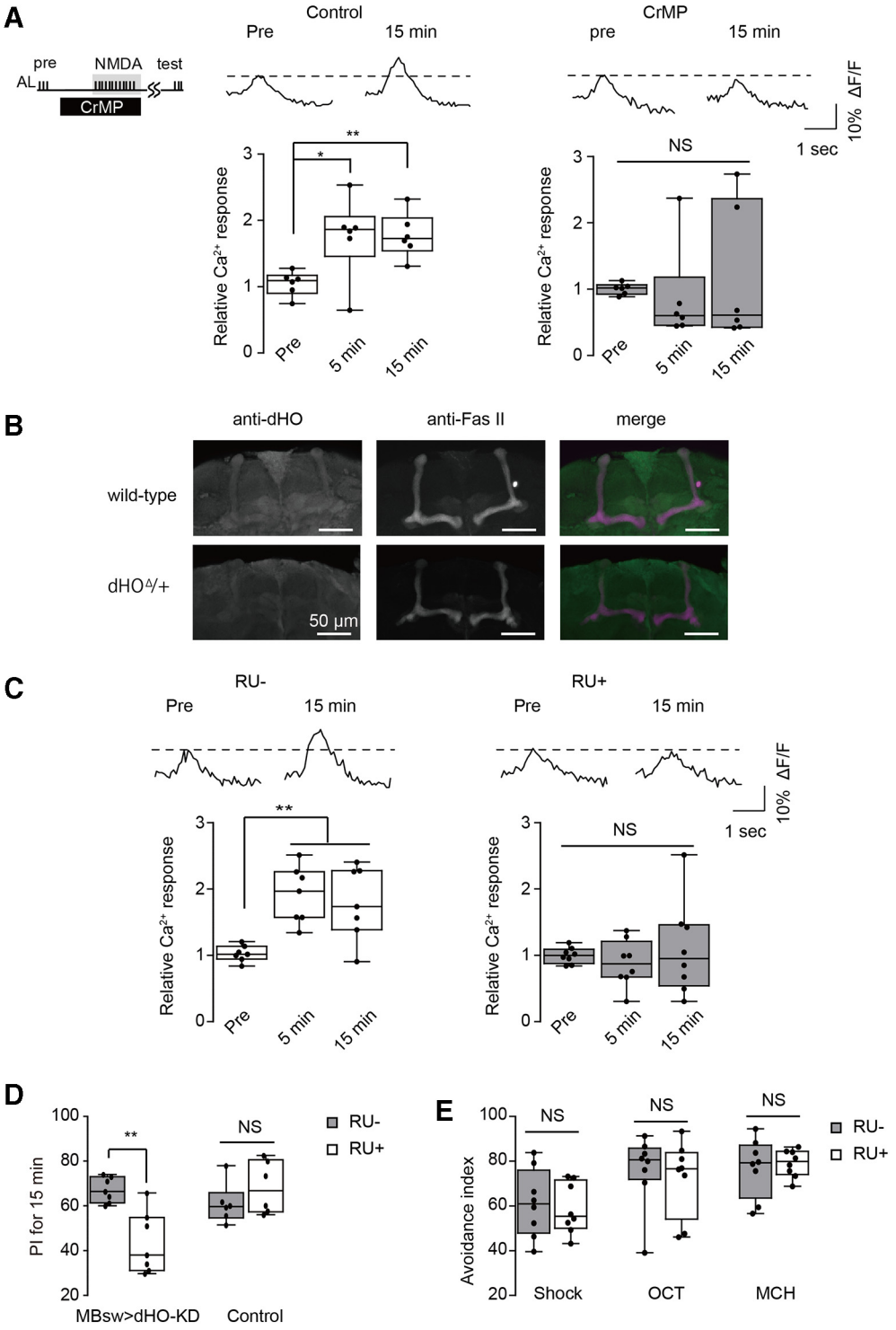

Figure 3. *dHO* in the MBs is required LTE and olfactory learning. ***A***, An HO inhibitor, CrMP, prevents LTE induced by AL+ NMDA stimulation. One-way ANOVA and Bonferroni *post hoc* tests indicate significant changes in AL-evoked Ca^{2+} responses in the MB after AL + NMDA stimulation in control conditions ($F_{(2,15)} = 5.836$, $p = 0.013$, $N = 6$) but not in 10 μM CrMP-treated conditions ($F_{(2,18)} = 0.339$, $p = 0.717$, $N = 7$). ***B***, dHO antibody labels the MB lobes and midline cells in the *Drosophila* brain. Fas II antibody staining is included to identify subsets of the MB lobes. *dHO* signals are reduced in dHO^{Δ} hemizygotes ($dHO^{\Delta}/+$), demonstrating the specificity of the antibody. ***C***, Knockdown of *dHO* in the MBs impairs LTE induced by AL + NMDA stimulation. One-way ANOVA and Bonferroni *post hoc* tests indicate significant LTE in the MB after AL + NMDA stimulation in control (RU^{-}) conditions (left: $F_{(2,18)} = 9.630$, $p = 0.001$, $N = 7$), but not in *dHO*-knockdown (RU^{+}) conditions (right: $F_{(2,21)} = 0.444$, $p = 0.647$, $N = 8$). ***D***, Knocking down *dHO* in the MBs impairs olfactory learning. $^{**}p < 0.01$ (Student's *t* test). $N = 7$ for all data. ***E***, Naive responses to odors and electrical shock are not affected by knocking down *dHO* in the MBs ($p > 0.05$, Student's t test). $N = 8$ for all experiments.

To verify that SV exocytosis from TH-DA neuronal terminals is directly related to DA release, we used a genetically encoded DA probe, DA1m (Sun et al., 2018), and found that DA amounts increased specifically on coincident AL + NMDA stimulation, but not on AL or NMDA stimulation alone (Fig. 4*A*). Furthermore, the increase in DA was inhibited by CrMP (Fig. 4*B*). Together, our results indicate that dHO in the MBs is required for olfactory memory, MB plasticity, and DA release onto MBs.

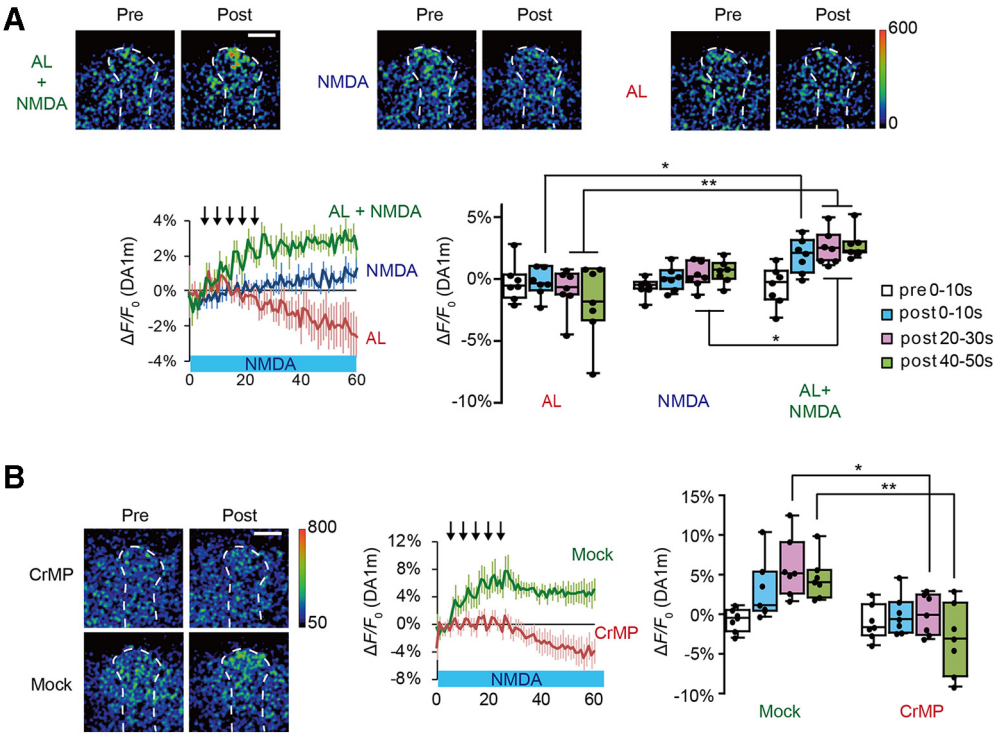

Figure 4. DA responses induced by coincident AL + NMDA stimulation are inhibited by a dHO inhibitor. ***A***, Top, Typical pseudo-color images of DA1m fluorescence in TH-DA terminals innervating the $\alpha 3/\alpha' 3$ compartments of the vertical MB lobes during AL + NMDA, NMDA, and AL stimulation experiments. The type of stimulation applied is indicated on the left, and responses before (pre) and after (post) stimulation are shown. Bottom left, Time course of DA1m changes on TH-DA terminals on indicated stimulations. Bottom right, Summary of DA1m fluorescence changes. Two-way ANOVA indicates significant differences in DA1m fluorescence due to stimulation type, time, and interaction between stimulation type and time ($F_{(6,72)} = 3.648$, $p = 0.0032$, $N = 7$ for all data). $^*p < 0.05$; $^{**}p < 0.01$; Bonferroni *post hoc* tests. ***B***, The HO inhibitor, CrMP, suppresses DA release as measured by DA1m fluorescence. Two-way ANOVA indicates significant differences in DA1m fluorescence due to drug treatment ($F_{(3,48)} = 3.716$, $p = 0.0175$, $N = 7$ for all data). $^*p < 0.05$; $^{**}p < 0.01$; Bonferroni *post hoc* tests.

CO generated from coincidentally activated MB neurons evokes DA release

If CO functions as a retrograde messenger inducing DA release, direct application of CO to DA terminals should induce release. Thus, we next applied CO-saturated saline from micropipettes to the vertical lobes of the MBs, and observed robust SV exocytosis from TH-DA terminals (Fig. 5*A*). Further, we found that application of CORM-3, a water-soluble CO-donor (Clark et al., 2003; Tinajero-Trejo et al., 2014; Aki et al., 2018), also evokes SV exocytosis from TH-DA terminals (Fig. 5*B*). In contrast, application of other retrograde messengers, including 200 μM arachidonic acid and 200 μM 2-arachidonylglycerol, an endocanabinoid receptor agonist, had no effects on release (Fig. 5*C*,*D*). To further examine whether endogenously generated CO is required for DA release, we used a CO selective scavenger, hemoCD (Kitagishi et al., 2010) and found that hemoCD significantly inhibited vesicular exocytosis from TH-DA terminals on AL + NMDA stimulation (Fig. 5*E*).

We next visualized the generation and release of CO from MB neurons using a CO-selective fluorescent probe, COP-1 (Michel et al., 2012; Ohata et al., 2019). While COP-1 fluorescence increased immediately after coincident AL + NMDA stimulation, fluorescence remained unchanged after AL stimulation or NMDA application alone (Fig. 6*A*). Thus, changes in COP-1 fluorescence parallel changes in DA release. Furthermore, the fluorescence increases in COP-1 occurred on the lobes of the MBs ipsilateral, but not contralateral, to the stimulated AL (Fig. 6*B*) when NMDA was bath-applied to both lobes of the brain and one AL was stimulated. Since each AL innervates its ipsilateral, but not contralateral MB, this suggests that CO production occurs in areas of coincident AL and NMDA activation. Again, this result parallels that of DA release (Ueno et al., 2017). Significantly, increased COP-1 fluorescence was attenuated by knocking down *dHO* in the MBs (Fig. 6*C*), indicating that COP-1 fluorescence detects dHO-dependent CO production. Collectively, these results suggest that coincident stimulation of MB neurons induces *dHO* to generate the retrograde messenger, CO, which then evokes SV exocytosis from presynaptic DA terminals.

While our results demonstrate that CO signaling is necessary and sufficient for DA release, we note that our studies use fluorescent reporters, which are not optimal for detailed kinetic analysis of release and reuptake. For example, increases in spH fluorescence can be used to determine vesicular release from DA neurons, but the decrease in spH fluorescence after release does not reflect the kinetics of clearance of DA from synaptic sites. Similarly, increases in COP-1 fluorescence reflect increases in CO production and release, but the kinetics of this increase depend on CO binding affinities and limits of detection (Fig. 6*D*). Thus, the gradual increase in COP-1 fluorescence following coincident activation does not indicate that CO production is similarly gradual. In addition, since COP-1 binding to CO is irreversible, we do not see a decrease in COP-1 fluorescence after the end of stimulation. Thus, although our functional imaging studies reliably measure significant changes in synaptic release, calcium signaling, and CO production, they are not precise enough to accurately measure the fast dynamics of these changes.

CO evokes noncanonical SV exocytosis

SV exocytosis requires an increase in Ca^{2+} concentration in presynaptic terminals (Katz and Miledi, 1967; Augustine et al., 1985; Sabatini and Regehr, 1996; Meinrenken et al., 2003). Consistent

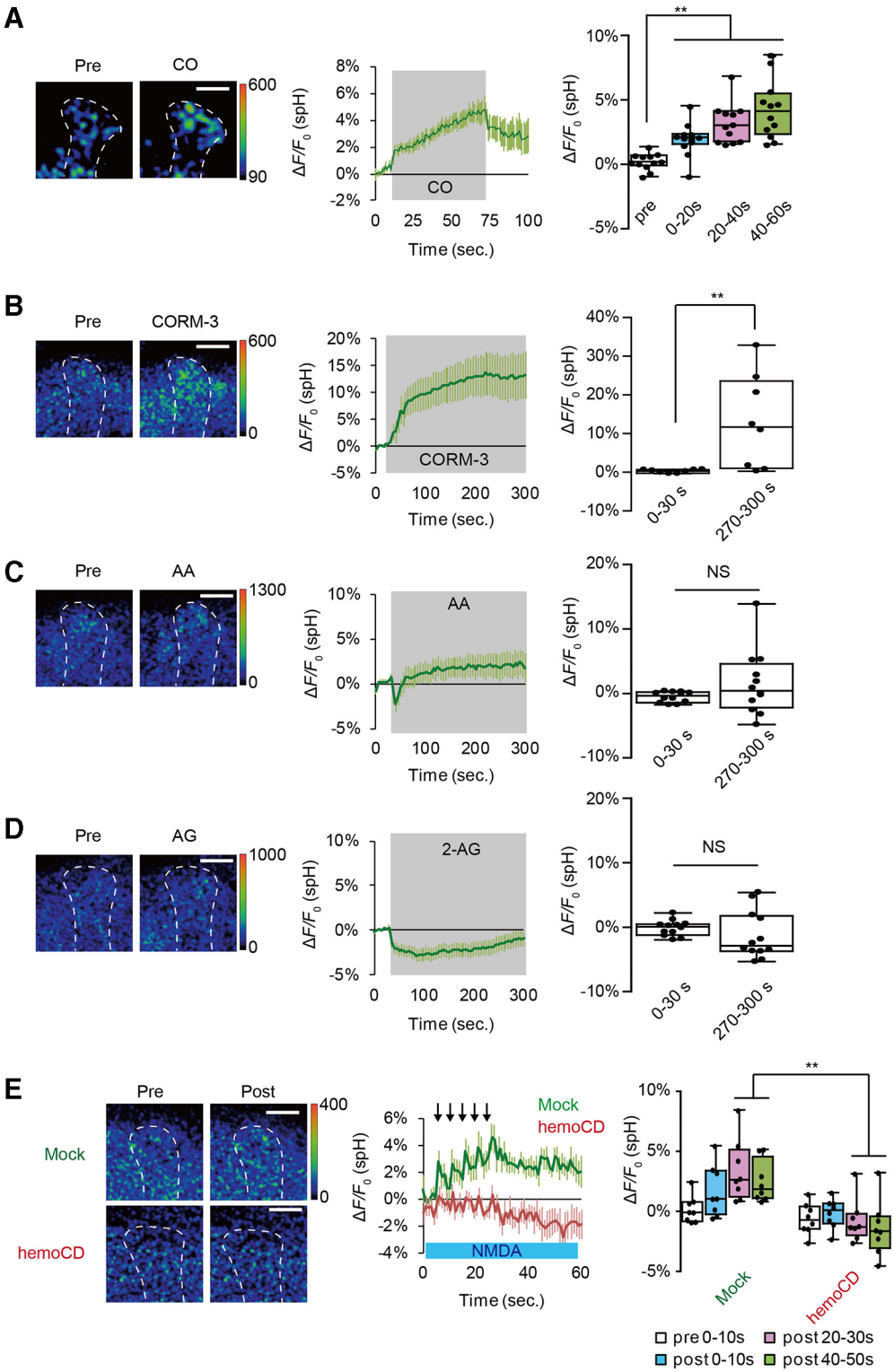

Figure 5. CO evokes SV exocytosis from DA terminals. ***A***, CO induces DA release. CO-saturated saline was puffed onto the vertical lobes of the MB during the indicated time period (middle, gray-shaded area). CO-induced spH responses were obtained by subtracting spH fluorescent changes induced by control N_2-satulated saline from fluorescence changes induced by CO-saturated saline. One-way ANOVA and *post hoc* tests indicate significant changes in spH fluorescence on CO application ($F_{(3,44)}$= 14.994, $p < 0.001$). $N = 12$ for all data. **$p < 0.01$ (Bonferroni *post hoc* tests). ***B***, CORM-3 induces DA release; 20 μM CORM-3 (dissolved in 0.2% DMSO) was bath-applied, and spH fluorescence was measured at DA terminals at the $\alpha3/\alpha'3$ compartments of the MB vertical lobes. CORM-3-induced spH responses were obtained by subtracting fluorescent changes induced by control 0.2% DMSO saline from fluorescence changes induced by CORM-3. **$p < 0.01$ (Student's *t* test), comparing spH responses before (0-30s) and after application of CO (270-300s). $N = 8$ for all data. ***C***, Arachidonic acid (AA) does not induce DA release; 200 μM AA (dissolved in 0.4% ethanol) was bath-applied. AA-induced spH responses were obtained by subtracting fluorescence changes induced by 0.4% ethanol saline from fluorescence changes induced by AA. Not significant ($p > 0.05$, Mann-Whitney test). $N = 16$ for all data. ***D***, Effects of 2-arachidonylglycerol (2-AG) on DA release; 200 μM AG (dissolved in 0.2% DMSO) was bath-applied. AG-induced spH responses were obtained by subtracting fluorescence changes induced by 0.2% DMSO saline from fluorescence changes induced by AG. Not significant ($p > 0.05$, Student's *t* test). $N = 12$ for all data. ***E***, The CO scavenger, hemoCD, prevents SV exocytosis from DA terminals. AL + NMDA-dependent changes in spH fluorescence were measured in the

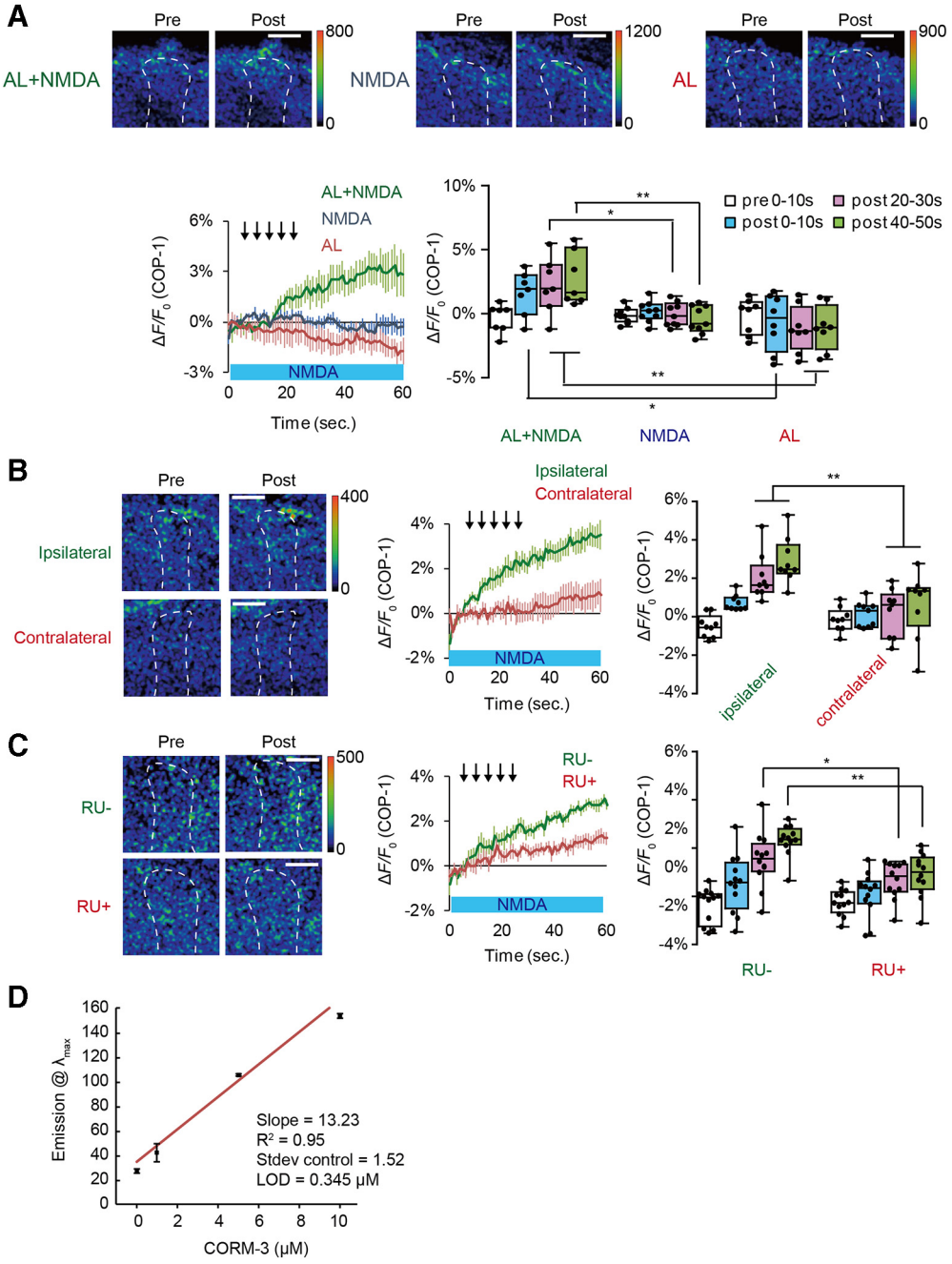

Figure 6. Endogenous CO released from MBs induces DA release. ***A***, Top panels, Typical images of COP-1 fluorescence observed at the $\alpha3/\alpha'3$ compartments of the MB vertical lobes. Pre, Images taken before stimulation; Post, images taken 30 s after onset of indicated stimuli. Bottom left, Time course of COP-1 fluorescence on indicated stimulation protocols. Bottom right, Summary of COP-1 fluorescence at different time intervals on indicated stimulation. Isolated brains were incubated in 4 μM COP-1, and COP-1 responses were calculated by subtracting nonstimulated fluorescence changes from stimulated fluorescence changes. In the COP-1 experiments, to accurately locate the MBs, we used transgenic flies expressing the red fluorescence Ca^{2+} indicator, R-GECO1, in the MBs. Two-way ANOVA indicates significant differences in COP-1 fluorescence due to treatment, time, and interaction between treatment and time ($F_{(6,84)} = 3.094$, $p = 0.0087$, $N = 8$ for AL or NMDA stimulation alone and $N = 7$ for AL + NMDA stimulation). $^*p < 0.05$; $^{**}p < 0.01$; Bonferroni *post hoc* tests. Scale bars, 20 μm. ***B***, CO is released from the MB lobe ipsilateral to AL stimulation. Two-way ANOVA indicates significant differences in fluorescence between MB lobes ($F_{(3,64)} = 5.491$, $p = 0.020$, $N = 9$ for all data). $^{**}p < 0.01$ (Bonferroni *post hoc* tests). ***C***, Knocking down *dHO* expression in the MBs impairs CO production. Two-way ANOVA indicates significant differences in COP-1 fluorescence due to RU treatment ($F_{(3,88)} = 6.25$, $p = 0.0086$, $N = 12$ for all data). $^{**}p < 0.01$ (Bonferroni *post hoc* tests). ***D***, Limit of detection (LOD) of COP-1 at 90 min determined by fluorescence intensity at 508 nm as a function of CORM-3 concentration. While LOD of COP-1 is 0.345 μM at 90 min, a similar range of LODs were found at other time points (LOD = 0.660 μM at $t = 30$ min, 0.673 μM at $t = 45$ min, 0.556 μM at $t = 60$ min). Each concentration was run in triplicate, and control was run 5 times. Data are mean ± SD.

←

presence and absence of 50 μM hemoCD. Two-way ANOVA indicates significant decreases in spH fluorescence due to hemoCD treatment ($F_{(3,56)} = 2.845$, $p = 0.0458$, $N = 8$ for all data). $^{**}p < 0.01$ (Bonferroni *post hoc* tests).

with this, we observed a robust Ca^{2+} increase in TH-DA terminals that project onto the MB lobes receiving coincident AL + NMDA stimulation (Fig. 7*A*), but not in terminals that project to the contralateral side (Fig. 7*B*). Ca^{2+} increases in DA terminals were also observed on application of CORM-3 (Fig. 7*C*), and this increase was abolished by addition of the membrane-permeable

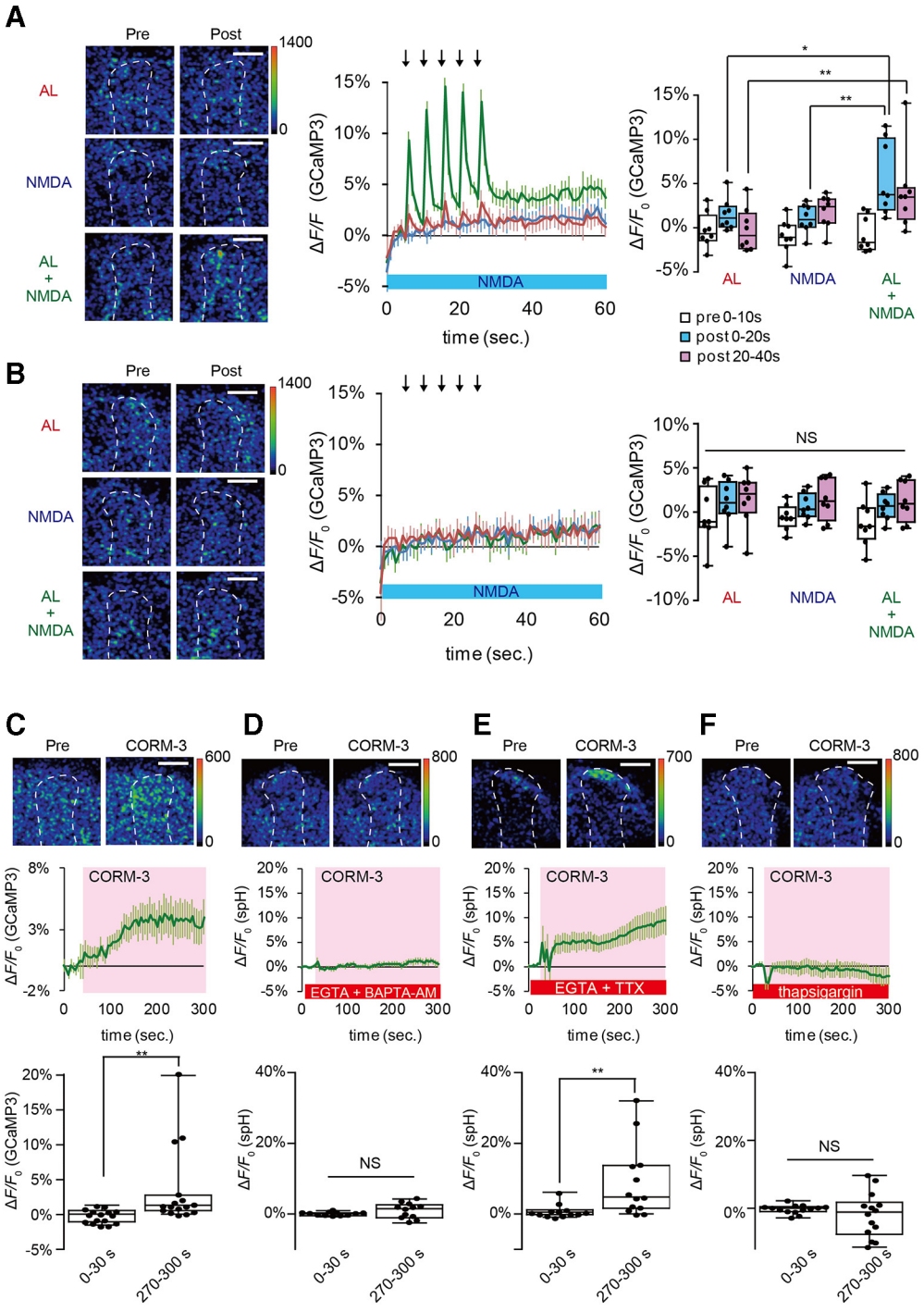

Figure 7. CO-induced DA release requires Ca^{2+} efflux from internal Ca^{2+} stores. ***A***, Left, Pseudo-color images of G-CaMP3 fluorescence in TH-DA terminals innervating the $\alpha3/\alpha'3$ compartments of the vertical MB lobes ipsilateral to the AL during AL, NMDA, and AL + NMDA stimulation. Left, The type of stimulation applied. Responses before (pre) and after (post) stimulation are shown. Middle, Time course of Ca^{2+} responses in TH-DA terminals on indicated stimulations. Right, Summary of responses. We expressed R-GECO1 in the MBs to help identify the $\alpha3/\alpha'3$ compartments of the MBs. Two-way ANOVA indicates significant differences in G-CaMP3 fluorescence due to stimulation type, time, and interaction between stimulation type and time ($F_{(4,63)} = 2.610$, $p = 0.0437$, $N = 8$ for all data). *$p < 0.05$; **$p < 0.01$; Bonferroni *post hoc* tests. ***B***, G-CaMP3 fluorescence changes in TH-DA terminals innervating the MB contralateral to the AL, on AL, NMDA, and AL + NMDA stimulation. Panels are similar to those shown in ***A***. Two-way ANOVA indicates no significant differences in G-CaMP3 fluorescence due to time or stimulation type. $N = 9$ for all data. ***C***, CORM-3 induces Ca^{2+} increases in TH-DA terminals. CORM-3 induced Ca^{2+} changes were calculated by subtracting fluorescence changes under mock conditions from changes induced by CORM-3; 20 μM CORM-3 (dissolved in 0.2% DMSO saline) was puffed onto the $\alpha3/\alpha'3$ compartments of the vertical MB lobes during the indicated time period (middle, pink). **$p < 0.01$ (Mann-Whitney test). $N = 16$ for all data. ***D***, CORM-3-induced DA release depends on increases in intracellular Ca^{2+}. Brains were incubated in Ca^{2+}-free external solution containing 2 mM EGTA and 10 μM BAPTA-AM for 10 min before CORM-3 application. $p = 0.166$ (Student's *t* test). $N = 12$. ***E***, CORM-3-induced DA release does not require influx of external Ca^{2+} or activity of voltage-gated Na^+ channels. Brains were placed in Ca^{2+}-free external solution containing 5 mM EGTA and 10 μM TTX 10 min before CORM-3 application. **$p < 0.01$ (Mann-Whitney test). $N = 13$. ***F***, CORM-3-induced DA release requires efflux from internal Ca^{2+} stores. Brains were incubated in Ca^{2+}-free external solution containing 10 μM thapsigargin for 10 min before CORM-3 application. $p = 0.364$ (Student's *t* test). $N = 14$.

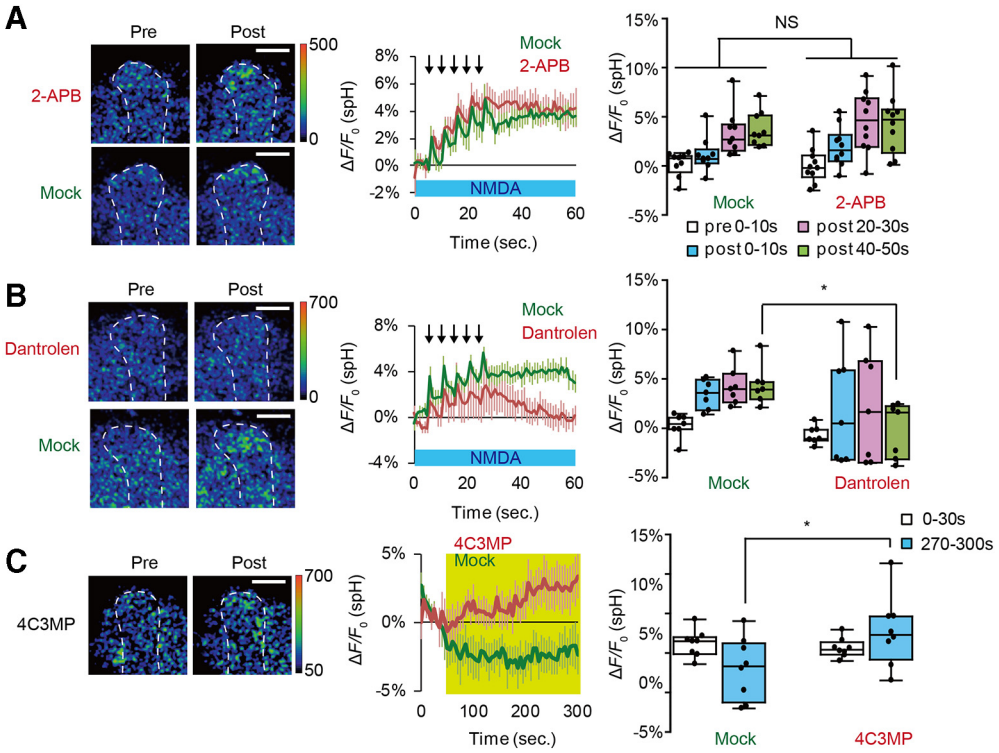

Figure 8. SV exocytosis from DA terminals induced by coincident AL + NMDA stimulation requires RyR. ***A***, An IP_3R inhibitor does not affect DA release; 100 μM 2-aminoethoxydiphenylborane (2-APB) was dissolved in 0.1% DMSO saline. Two-way ANOVA indicates no significant differences in spH fluorescence due to 2-APB treatment. $N = 10$ for 2-APB treatment and $N = 9$ for mock control. ***B***, The RyR inhibitor, dantrolene, inhibits DA release; 10 μM dantrolene was dissolved in 0.1% DMSO saline. Two-way ANOVA indicates significant effects of drug treatment on spH fluorescence ($F_{(1,48)} = 6.781$, $p = 0.0122$, $N = 8$ for all data). *$p < 0.05$ compared with mock-treated samples assayed (Bonferroni *post hoc* tests). ***C***, Application of a RyR agonist induces DA release. 4-Chloro-3-methylphenol (4C3MP) was dissolved at 1 mM in 0.2% ethanol saline containing 1 μM TTX and applied for the indicated period of time (yellow). Two-way ANOVA indicates significant effects of drug treatment on spH fluorescence ($F_{(1,28)} = 5.466$, $p = 0.027$). $N = 8$ for all data. *$p < 0.05$ (Bonferroni *post hoc* tests).

Ca^{2+} chelator BAPTA-AM (Fig. 7*D*). In canonical SV exocytosis, neuronal activity opens voltage-gated calcium channels, allowing influx of extracellular Ca^{2+} (Katz and Miledi, 1967; Augustine et al., 1985). However, we found that CORM-3 is able to induce SV exocytosis from TH-DA terminals, even in Ca^{2+} free saline in the presence of the Ca^{2+} chelator, EGTA, and the sodium channel blocker, TTX (Fig. 7*E*). This suggests that CO-evoked DA release is action potential-independent and does not require Ca^{2+} influx from extracellular sources.

Since extracellular Ca^{2+} is not responsible for CO-dependent DA release, we next examined whether Ca^{2+} efflux from internal stores may be required. Significantly, CORM-3 failed to increase Ca^{2+} in TH-DA terminals in the presence of EGTA and thapsigargin, an inhibitor of the sarcoplasmic/endoplasmic reticulum Ca^{2+} ATPase, which depletes internal Ca^{2+} stores (Kijima et al., 1991; Sagara and Inesi, 1991) (Fig. 7*F*). Thus, CO-evoked DA release occurs through a noncanonical mechanism that depends on Ca^{2+} efflux from internal stores rather than from extracellular sources.

RyRs mediate $Ca2^{+}$ efflux for CO-evoked DA release

What mediates Ca^{2+} efflux from internal stores in DA terminals? Inositol 1,4,5-trisphosphate receptors (IP_3Rs) and RyRs are the major channels mediating Ca^{2+} release from internal stores (Bardo et al., 2006). While SV exocytosis evoked by coincident MB stimulation was not suppressed by 2-aminoethoxydiphenyl borate, an IP_3R antagonist (Maruyama et al., 1997) (Fig. 8*A*), exocytosis was significantly inhibited by dantrolene, a RyR antagonist (Zhao et al., 2001) (Fig. 8*B*). Conversely, application of a RyR agonist, 4-chloro-3-methylphenol (Zorzato et al., 1993) was sufficient to evoke exocytosis (Fig. 8*C*). These data suggest that RyR in DA neurons are required for SV exocytosis on coincident activation of MB neurons.

To address whether *RyR* is expressed in DA terminals, we examined expression of mCD8::GFP in *Mi{Trojan-GAL4.0}* $RyR^{MI08146\text{-}TG4.0}$*; P{UAS-mCD8::GFP}* flies. In *Mi{Trojan-GAL4.0}* $RyR^{MI08146\text{-}TG4.0}$, a Trojan GAL4 exon is inserted between exons 18 and 19 in the same orientation as the *RyR* gene (Diao et al., 2015). Thus, GAL4, and mCD8::GFP, expression should reflect *RyR* expression. In these flies, mCD8::GFP signals overlapped with anti-TH antibody signals, indicating that RyR is expressed in DA neurons (Fig. 9*A*). To determine whether RyR are acutely required for DA release, we used the TARGET system (McGuire et al., 2003) to knock down *RyR* in adult TH-DA neurons, and found that this significantly suppressed SV exocytosis from DA terminals on AL + NMDA stimulation (Fig. 9*B*). Furthermore, knockdown of *RyRs* is suppressed SV exocytosis induced by direct CO application to TH-DA terminals (Fig. 9*C*), and also suppressed LTE on coincident AL + NMDA stimulation (Fig. 9*D*). Finally, we tested whether *RyR* in TH-DA neurons are required for olfactory memory, and found that knocking down of *RyRs* in TH-DA neurons impaired short-term olfactory memory (1 h memory after training) (Fig. 9*E*), without affecting odor and shock response (Fig. 9*F*). Thus, presynaptic RyR are required for activation-dependent and CO-dependent DA release, MB plasticity, and olfactory memory.

Discussion

CO functions as a retrograde on-demand messenger for SV exocytosis in presynaptic DA terminals

A central tenet of neurobiology is that action potentials, propagating from the cell bodies, induce Ca^{2+} influx in presynaptic

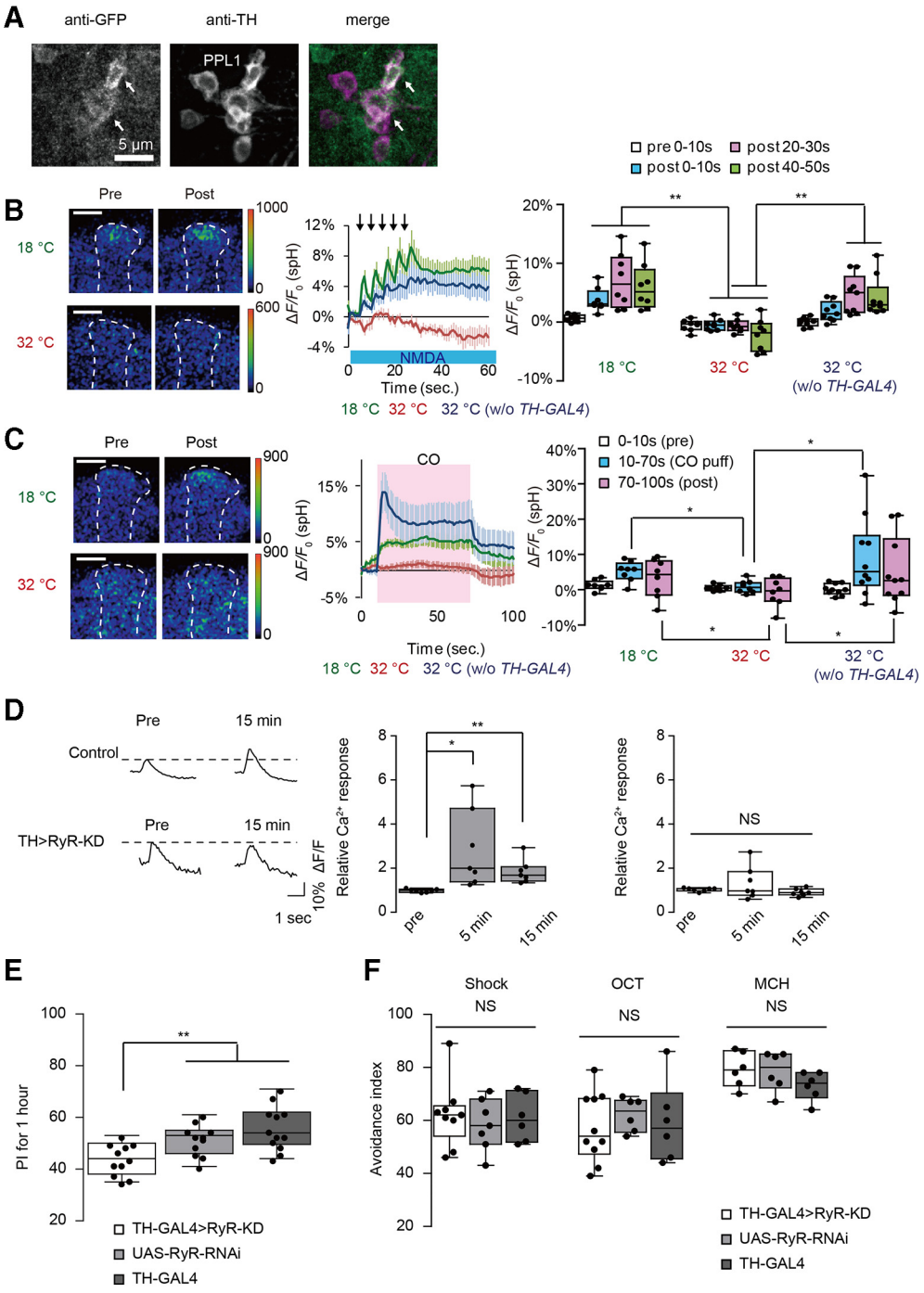

Figure 9. CO-induced DA release is mediated by RyRs. ***A***, RyR localization was examined in *UAS-mCD8::GFP/Mi{Trojan-GAL4.0} RyR[MI08146-TG4.0]* flies in which expression of *mCD8::GFP* is driven by Trojan-GAL4 inserted in the endogenous *RyR* gene. GFP expression overlapped with expression of TH in PPL1 DA neurons (arrows) that innervate the vertical lobes of the MBs. ***B***, Temporal *RyR* knockdown at 32°C in TH-DA neurons prevents DA release evoked by AL + NMDA stimulation. Two-way ANOVA indicates significant differences in spH fluorescence between restrictive and permissive temperatures ($F_{(3,56)} = 6.625$, $p = 0.0007$, $N = 8$ for all data). $^{**}p < 0.01$ (Bonferroni *post hoc* tests). ***C***, Temporal knockdown of *RyR* in TH-DA neurons prevents DA release evoked by CO application. CO-saturated saline was applied during the indicated time period (pink) from a micropipette. Two-way ANOVA indicates significant interaction differences in spH fluorescence due to time, temperature, and interaction between time and temperature ($F_{(2,42)} = 12.6$, $p < 0.0001$, $N = 8$ for all data). $^{**}p < 0.01$ (Bonferroni *post hoc* tests). ***D***, Knocking down *RyR* in TH-DA neurons abolishes LTE induced by AL + NMDA stimulation. One-way ANOVA and Bonferroni *post hoc* tests indicate significant increases in AL-evoked Ca^{2+} responses after AL + NMDA stimulation in control brains ($F_{(2,18)} = 5.455$, $p = 0.014$) but not in *TH>RyR-KD* brains ($F_{(2,18)} = 1.666$, $p = 0.217$). $N = 7$ for all data. ***E***, Knocking down *RyR* in TH-DA neurons impairs 1 h olfactory memory ($F_{(2,28)} = 7.735$, $p = 0.002$). $^{*}p < 0.01$ (Bonferroni *post hoc* tests). $N = 11$ for *TH-GAL4>RyR-KD* and *UAS-RyR RNAi*, and $N = 12$ for *TH-GAL4*. ***F***, Naive responses to odors and electrical shock are not affected by knocking down *RyR* in TH-DA neurons (Shock: $F_{(2,19)} = 1.213$, $p = 0.319$, $N = 9$ for *TH-GAL4>RyR-KD*, $N = 7$ for *UAS-RyR RNAi*, and $N = 6$ for *TH-GAL4*; OCT: $F_{(2,19)} = 1.564$, $p = 0.235$, $N = 10$ for *TH-GAL4>RyR-KD*, $N = 6$ for *UAS-RyR RNAi* and *TH-GAL4*; MCH: $F_{(2,15)} = 0.669$, $p = 0.527$, $N = 6$ for all genotypes).

terminals to evoke SV exocytosis. However, recent mammalian studies have shown that only a certain fraction of a large number of presynaptic DA release sites is involved in canonical SV exocytosis (Pereira et al., 2016; Liu et al., 2018). In this study, we identify a novel mechanism of SV exocytosis in which activity in postsynaptic neurons evokes presynaptic release to induce plastic changes. This mechanism allows the timing and location of DA release to be strictly defined by activity of postsynaptic neurons.

On-demand SV exocytosis uses CO as a retrograde signal from postsynaptic MB neurons to presynaptic DA terminals. We demonstrate that CO fulfills the criteria that have been proposed for a retrograde messenger (Regehr et al., 2009). First, we demonstrate that HO, which catalyzes CO production, is highly expressed in postsynaptic MB neurons, indicating that MB neurons have the capacity to synthesize the messenger. Second, we show that pharmacological and genetic suppression of HO activity in the MBs inhibits CO production, presynaptic DA release, and LTE. Third, using a CO fluorescent probe, COP-1 (Michel et al., 2012), we demonstrate that CO is generated in the MBs following coincident stimulation of the MBs, and CO generation is restricted to lobes of MB neurons that receive coincident stimulation. We further show that direct application of CO, or a CO donor, induces DA release from presynaptic terminals, whereas addition of a CO scavenger, HemoCD, suppresses release. Fourth, we demonstrate that CO activates RyR in presynaptic terminals to induce SV exocytosis. Strikingly, CO-dependent SV exocytosis does not depend on influx of extracellular Ca^{2+} but instead requires efflux of Ca^{2+} from internal stores via RyR. Finally, we show that pharmacological inhibition and genetic suppression of RyR in DA neurons impair DA release after coincident stimulation and CO application.

Other retrograde signals, such as NO and endocannabinoids, enhance or suppress canonical SV exocytosis, but we find that CO-dependent DA release occurs even in conditions that block neuronal activity and Ca^{2+} influx in presynaptic DA terminals. This suggests that CO does not function to modulate canonical SV exocytosis, but may instead evoke exocytosis through a novel mechanism. Several previous studies have indicated that CO and RyR-dependent DA release also occurs in mammals. A microdialysis study has shown that CO increases the extracellular DA concentration in the rat striatum and hippocampus (Hiramatsu et al., 1994), either through increased DA release or inhibition of DA reuptake (Taskiran et al., 2003). Also, pharmacological stimulation of RyRs has been reported to induce DA release in the mice striatum (Oyamada et al., 1998; Wan et al., 1999). This release is attenuated in RyR3-deficient mice, while KCl-induced DA release, which requires influx of extracellular Ca^{2+}, is unaffected, suggesting that RyR-dependent release is distinct from canonical DA release. However, it has been unknown whether and how CO is generated endogenously. Physiologic conditions that activate RyR to evoke DA release have also been unclear.

Signaling pathway for CO-dependent on-demand release of DA

While most neurotransmitters are stored in synaptic vesicles and released on neuronal depolarization, the release of gaseous retrograde messengers, such as NO and CO, is likely coupled to activation of their biosynthetic enzymes, NOS and HO. In mammals, an HO isoform, HO-2, is selectively enriched in neurons, and HO-2-derived CO is reported to function in plasticity. HO-2 is activated by Ca^{2+}/calmodulin (CaM) binding (Boehning et al., 2004), and by casein kinase II (CKII) phosphorylation (Boehning et al., 2003). Previously, we showed that coincident AL + NMDA stimulation induces a robust Ca^{2+} increase in the MBs that is greater than the increase from either stimulation alone (Ueno et al., 2017). We propose that this increase may activate *Drosophila* HO in the MB to generate CO during associative stimulation.

While *Drosophila* has a single isoform of RyR, mammals have three isoforms, RyR1-RyR3. Skeletal muscle and cardiac muscle primarily express RyR1 and RyR2, and the brain, including the striatum, hippocampus, and cortex, expresses all three isoforms (Giannini et al., 1995). RyRs are known to be activated by Ca^{2+} to mediate Ca^{2+} induced Ca^{2+} release (Endo, 2009). However, CO-evoked DA release occurs even in the presence of Ca^{2+}-free extracellular solutions containing TTX and EGTA, suggesting that CO activates RyR through a different mechanism. In addition to Ca^{2+}, RyR can be activated by calmodulin, ATP, PKA, PKG, cADP-ribose, and NO (Takasago et al., 1991; Xu et al., 1998; Verkhratsky, 2005; Zalk et al., 2007; Lanner et al., 2010; Kakizawa, 2013). NO can directly stimulate RyR1 nonenzymatically by S-nitrosylating a histidine residue to induce Ca^{2+} efflux (Xu et al., 1998; Kakizawa, 2013). CO has been reported to activate Ca^{2+}-activated potassium channels (K_{Ca}) through a nonenzymatic reaction in rat artery smooth muscle (Wang and Wu, 2003), raising the possibility that it may activate RyR through a similar mechanism. Alternatively, both NO and CO can bind to the heme moiety of soluble guanlylate cyclase leading to its activation (Stone and Marletta, 1994). Activated soluble guanlylate cyclase produces cGMP, and cGMP-dependent protein kinase (PKG) rapidly phosphorylates and activates RyRs (Takasago et al., 1991). Interestingly, NO increases DA in the mammalian striatum in a neural activity-independent manner (Hanbauer et al., 1992; Zhu and Luo, 1992; Lonart et al., 1993). Since activation of RyRs also increases extracellular DA in the striatum, hippocampus, and cortex (Oyamada et al., 1998; Wan et al., 1999), NO may play a pivotal role in RyRs activation and DA release in mammals. However, NOS expression has not been detected in the MBs (Muller, 1994; Regulski and Tully, 1995), suggesting that, in *Drosophila*, CO rather than NO may function in this process.

Glutamate signaling during association

In previous studies, we showed that electrical activity from the AL and AFV is transmitted to the MBs by cholinergic and glutamatergic neurons acting on nAChRs and NMDARs, respectively (Ueno et al., 2017). Although the cholinergic inputs from the AL are known to be delivered by projection neurons (Yasuyama et al., 2002; Su and O'Dowd, 2003), the glutamate inputs are still unclear. We previously identified glutamatergic neurons that innervate $\alpha3/\alpha'3$ compartments of the MBs, and that show SV release on electrical stimulation of the AFV (Ueno et al., 2017). We propose that these neurons may transmit information regarding AFV stimuli to the MBs. Alternatively, while NMDARs are localized throughout MB lobes (Miyashita et al., 2012), vesicular glutamate transporter-positive terminals are found only sparsely on the MBs (Sinakevitch et al., 2010). This suggests that neurons expressing a currently uncharacterized vesicular glutamate transporter may convey information from the AFV to MBs.

Biological significance of on-demand DA release

DA plays a critical role in associative learning and synaptic plasticity (Huang and Kandel, 1995; Jay, 2003; Puig et al., 2014; Lee et al., 2017; Yamasaki and Takeuchi, 2017). In flies, neutral odors induce MB responses by activating sparse subsets of MB neurons. After being paired with electrical shocks during aversive olfactory conditioning, odors induce larger MB responses in certain areas of the MBs (Yu et al., 2006; Wang et al., 2008; Akalal et al., 2011; Davis, 2011). We modeled this plastic change in *ex vivo* brains as LTE, and showed that DA application alone is sufficient to induce this larger response (Ueno et al., 2017). However, in the *Drosophila* brain, only a small number of DA neurons (~12 for aversive and ~100 for appetitive) regulate plasticity in ~2000 MB Kenyon cells (Mao and Davis, 2009). Thus, to form odor-specific associations, there should be a

mechanism regulating release at individual synapses. CO-dependent on-demand DA release provides this type of control. If on-demand release is involved in plasticity and associative learning, knockdown of genes associated with release should affect learning. Indeed, we show that knocking down either *dHO* in the MBs or *RyR* in DA neurons impairs olfactory conditioning. While these knockdowns did not completely abolish olfactory conditioning, this may be due to inefficiency of our knockdown lines. Alternatively, on-demand release may not be the only mechanism responsible for memory formation, but may instead be required for a specific phase of olfactory memory.

In our *ex vivo* studies, we find that DA release requires coincident activation of postsynaptic MB neurons by cholinergic and glutamatergic stimuli. However, other *in vivo* imaging studies have shown that DA neurons can be activated and release DA on odor stimulation or shock application alone (Dylla et al., 2017; Sun et al., 2018). Notably, projection of DA terminals is compartmentalized on the MB lobes and shows distinct responses and DA release during sensory processing (Cohn et al., 2015; Sun et al., 2018). In our studies, we examined dopaminergic neurons innervating the the $\alpha3/\alpha'3$ compartments at the tips of the MB vertical lobes, whereas other studies focused on compartments located on the MB horizontal lobes (Dylla et al., 2017; Sun et al., 2018). This suggests that plasticity in different MB compartments may be regulated by different mechanisms. Unfortunately, due the location of the microelectrode for AL stimulation which caused interference in fluorescent imaging of the horizontal lobes, we could not obtain reliable imaging data from these lobes in this study. Another difference between *ex vivo* and *in vivo* studies is that *in vivo* imaging studies use living, tethered, dissected flies that are likely in different states of arousal/distress, are exposed to many different stimuli, and can form unintended associations. In contrast, brains in *ex vivo* preparations are in a more controlled environment and are likely exposed to fewer unintended sensory stimuli. This may also explain apparent discrepancies between our *ex vivo* and pervious *in vivo* results.

In mammals, the role of CO in synaptic plasticity is unclear. Application of CO paired with low-frequency stimulation induces LTP, while inhibiting HO blocks LTP in the CA1 region of the hippocampus (Zhuo et al., 1993). However, HO-2-deficient mice have been reported to have normal hippocampal CA1 LTP (Poss et al., 1995). In contrast to CO, a role for NO in synaptic plasticity and learning has been previously reported (Muller, 1996; Balaban et al., 2014; Korshunova and Balaban, 2014). Thus, at this point, it is an open question whether CO or NO evokes DA release in mammals. Downstream from CO or NO, RyRs have been shown to be required for hippocampal and cerebellar synaptic plasticity (Wang et al., 1996; Balschun et al., 1999; Lu and Hawkins, 2002; Kakizawa et al., 2012).

Our current results suggest that DA neurons release DA via two distinct mechanisms: canonical exocytosis and on-demand release. Canonical exocytosis is evoked by electrical activity of presynaptic DA neurons, requires Ca^{2+} influx, and may be involved in volume transmission. This mode of release can activate widespread targets over time, and is suited for regulating global brain functions. In contrast, on-demand release is evoked by activity of postsynaptic neurons, requires Ca^{2+} efflux via *RyR*, and can regulate function of specific targets at precise times. DA neurons may differentially use these two modes of SV exocytosis in a context-dependent manner. Understanding how DA neurons differentially use these modes of transmission will provide new insights into how a relatively small number of DA neurons can control numerous different brain functions.

References

Agnati LF, Zoli M, Stromberg I, Fuxe K (1995) Intercellular communication in the brain: wiring versus volume transmission. Neuroscience 69:711–726.

Akalal DB, Yu D, Davis RL (2011) The long-term memory trace formed in the *Drosophila* alpha/beta mushroom body neurons is abolished in long-term memory mutants. J Neurosci 31:5643–5647.

Aki T, Unuma K, Noritake K, Kurahashi H, Funakoshi T, Uemura K (2018) Interaction of carbon monoxide-releasing ruthenium carbonyl CORM-3 with plasma fibronectin. Toxicol In Vitro 50:201–209.

Alkadhi KA, Al-Hijailan RS, Malik K, Hogan YH (2001) Retrograde carbon monoxide is required for induction of long-term potentiation in rat superior cervical ganglion. J Neurosci 21:3515–3520.

Aso Y, Grubel K, Busch S, Friedrich AB, Siwanowicz I, Tanimoto H (2009) The mushroom body of adult *Drosophila* characterized by GAL4 drivers. J Neurogenet 23:156–172.

Aso Y, Siwanowicz I, Bracker L, Ito K, Kitamoto T, Tanimoto H (2010) Specific dopaminergic neurons for the formation of labile aversive memory. Curr Biol 20:1445–1451.

Aso Y, Herb A, Ogueta M, Siwanowicz I, Templier T, Friedrich AB, Ito K, Scholz H, Tanimoto H (2012) Three dopamine pathways induce aversive odor memories with different stability. PLoS Genet 8:e1002768.

Aso Y, Sitaraman D, Ichinose T, Kaun KR, Vogt K, Belliart-Guérin G, Plaçais PY, Robie AA, Yamagata N, Schnaitmann C, Rowell WJ, Johnston RM, Ngo TT, Chen N, Korff W, Nitabach MN, Heberlein U, Preat T, Branson KM, Tanimoto H, et al. (2014) Mushroom body output neurons encode valence and guide memory-based action selection in *Drosophila*. Elife 3:e04580.

Augustine GJ, Charlton MP, Smith SJ (1985) Calcium entry and transmitter release at voltage-clamped nerve terminals of squid. J Physiol 367:163–181.

Balaban PM, Roshchin M, Timoshenko AK, Gainutdinov KL, Bogodvid TK, Muranova LN, Zuzina AB, Korshunova TA (2014) Nitric oxide is necessary for labilization of a consolidated context memory during reconsolidation in terrestrial snails. Eur J Neurosci 40:2963–2970.

Balschun D, Wolfer DP, Bertocchini F, Barone V, Conti A, Zuschratter W, Missiaen L, Lipp HP, Frey JU, Sorrentino V (1999) Deletion of the ryanodine receptor type 3 (RyR3) impairs forms of synaptic plasticity and spatial learning. EMBO J 18:5264–5273.

Bardo S, Cavazzini MG, Emptage N (2006) The role of the endoplasmic reticulum Ca^{2+} store in the plasticity of central neurons. Trends Pharmacol Sci 27:78–84.

Boehning D, Sedaghat L, Sedlak TW, Snyder SH (2004) Heme oxygenase-2 is activated by calcium-calmodulin. J Biol Chem 279:30927–30930.

Boehning D, Moon C, Sharma S, Hurt KJ, Hester LD, Ronnett GV, Shugar D, Snyder SH (2003) Carbon monoxide neurotransmission activated by CK2 phosphorylation of heme oxygenase-2. Neuron 40:129–137.

Boultadakis A, Pitsikas N (2010) Effects of the nitric oxide synthase inhibitor L-NAME on recognition and spatial memory deficits produced by different NMDA receptor antagonists in the rat. Neuropsychopharmacology 35:2357–2366.

Cervantes-Sandoval I, Phan A, Chakraborty M, Davis RL (2017) Reciprocal synapses between mushroom body and dopamine neurons form a positive feedback loop required for learning. Elife 6:e23789.

Claridge-Chang A, Roorda RD, Vrontou E, Sjulson L, Li H, Hirsh J, Miesenböck G (2009) Writing memories with light-addressable reinforcement circuitry. Cell 139:405–415.

Clark JE, Naughton P, Shurey S, Green CJ, Johnson TR, Mann BE, Foresti R, Motterlini R (2003) Cardioprotective actions by a water-soluble carbon monoxide-releasing molecule. Circ Res 93:e2–e8.

Cohn R, Morantte I, Ruta V (2015) Coordinated and compartmentalized neuromodulation shapes sensory processing in *Drosophila*. Cell 163:1742–1755.

Cui L, Yoshioka Y, Suyari O, Kohno Y, Zhang X, Adachi Y, Ikehara S, Yoshida T, Yamaguchi M, Taketani S (2008) Relevant expression of *Drosophila* heme oxygenase is necessary for the normal development of insect tissues. Biochem Biophys Res Commun 377:1156–1161.

Cypionka H, Meyer O (1983) Carbon monoxide-insensitive respiratory chain of *Pseudomonas carboxydovorans*. J Bacteriol 156:1178–1187.

Davis RL (2011) Traces of *Drosophila* memory. Neuron 70:8–19.

Diao F, Ironfield H, Luan H, Diao F, Shropshire WC, Ewer J, Marr E, Potter CJ, Landgraf M, White BH (2015) Plug-and-play genetic access to

Drosophila cell types using exchangeable exon cassettes. Cell Rep 10:1410–1421.

Dubnau J, Grady L, Kitamoto T, Tully T (2001) Disruption of neurotransmission in *Drosophila* mushroom body blocks retrieval but not acquisition of memory. Nature 411:476–480.

Dura JM, Preat T, Tully T (1993) Identification of linotte, a new gene affecting learning and memory in *Drosophila melanogaster*. J Neurogenet 9:1–14.

Dylla KV, Raiser G, Galizia CG, Szyszka P (2017) Trace conditioning in *Drosophila* induces associative plasticity in mushroom body Kenyon cells and dopaminergic neurons. Front Neural Circuits 11:42.

Endo M (2009) Calcium-induced calcium release in skeletal muscle. Physiol Rev 89:1153–1176.

Friggi-Grelin F, Coulom H, Meller M, Gomez D, Hirsh J, Birman S (2003) Targeted gene expression in *Drosophila* dopaminergic cells using regulatory sequences from tyrosine hydroxylase. J Neurobiol 54:618–627.

Gerber B, Tanimoto H, Heisenberg M (2004) An engram found? Evaluating the evidence from fruit flies. Curr Opin Neurobiol 14:737–744.

Giannini G, Conti A, Mammarella S, Scrobogna M, Sorrentino V (1995) The ryanodine receptor/calcium channel genes are widely and differentially expressed in murine brain and peripheral tissues. J Cell Biol 128:893–904.

Goncharenko K, Eftekharpour E, Velumian AA, Carlen PL, Fehlings MG (2014) Changes in gap junction expression and function following ischemic injury of spinal cord white matter. J Neurophysiol 112:2067–2075.

Gu H, O'Dowd DK (2007) Whole cell recordings from brain of adult *Drosophila*. J Vis Exp 6:248.

Hanbauer I, Wink D, Osawa Y, Edelman GM, Gally JA (1992) Role of nitric oxide in NMDA-evoked release of [3H]-dopamine from striatal slices. Neuroreport 3:409–412.

Hiramatsu M, Yokoyama S, Nabeshima T, Kameyama T (1994) Changes in concentrations of dopamine, serotonin, and their metabolites induced by carbon monoxide (CO) in the rat striatum as determined by in vivo microdialysis. Pharmacol Biochem Behav 48:9–15.

Horiuchi J (2019) Recurrent loops: incorporating prediction error and semantic/episodic theories into *Drosophila* associative memory models. Genes Brain Behav 18:e12567.

Huang YY, Kandel ER (1995) D1/D5 receptor agonists induce a protein synthesis-dependent late potentiation in the CA1 region of the hippocampus. Proc Natl Acad Sci USA 92:2446–2450.

Ichinose T, Aso Y, Yamagata N, Abe A, Rubin GM, Tanimoto H (2015) Reward signal in a recurrent circuit drives appetitive long-term memory formation. Elife 4:e10719.

Iliadi KG, Avivi A, Iliadi NN, Knight D, Korol AB, Nevo E, Taylor P, Moran MF, Kamyshev NG, Boulianne GL (2008) nemy encodes a cytochrome b561 that is required for *Drosophila* learning and memory. Proc Natl Acad Sci USA 105:19986–19991.

Jacobitz S, Meyer O (1989) Removal of CO dehydrogenase from *Pseudomonas carboxydovorans* cytoplasmic membranes, rebinding of CO dehydrogenase to depleted membranes, and restoration of respiratory activities. J Bacteriol 171:6294–6299.

Jay TM (2003) Dopamine: a potential substrate for synaptic plasticity and memory mechanisms. Prog Neurobiol 69:375–390.

Kakizawa S (2013) Nitric oxide-induced calcium release: activation of type 1 ryanodine receptor, a calcium release channel, through non-enzymatic post-translational modification by nitric oxide. Front Endocrinol (Lausanne) 4:142.

Kakizawa S, Yamazawa T, Chen Y, Ito A, Murayama T, Oyamada H, Kurebayashi N, Sato O, Watanabe M, Mori N, Oguchi K, Sakurai T, Takeshima H, Saito N, Iino M (2012) Nitric oxide-induced calcium release via ryanodine receptors regulates neuronal function. EMBO J 31:417–428.

Katz B, Miledi R (1967) Ionic requirements of synaptic transmitter release. Nature 215:651.

Kijima Y, Ogunbunmi E, Fleischer S (1991) Drug action of thapsigargin on the Ca^{2+} pump protein of sarcoplasmic reticulum. J Biol Chem 266:22912–22918.

Kitagishi H, Negi S, Kiriyama A, Honbo A, Sugiura Y, Kawaguchi AT, Kano K (2010) A diatomic molecule receptor that removes CO in a living organism. Angew Chem Int Ed Engl 49:1312–1315.

Kitamoto T (2001) Conditional modification of behavior in *Drosophila* by targeted expression of a temperature-sensitive shibire allele in defined neurons. J Neurobiol 47:81–92.

Korshunova TA, Balaban PM (2014) Nitric oxide is necessary for long-term facilitation of synaptic responses and for development of context memory in terrestrial snails. Neuroscience 266:127–135.

Lanner JT, Georgiou DK, Joshi AD, Hamilton SL (2010) Ryanodine receptors: structure, expression, molecular details, and function in calcium release. Cold Spring Harb Perspect Biol 2:a003996.

Lee JH, Lee S, Kim JH (2017) Amygdala circuits for fear memory: a key role for dopamine regulation. Neuroscientist 23:542–553.

Liu C, Kershberg L, Wang J, Schneeberger S, Kaeser PS (2018) Dopamine secretion is mediated by sparse active zone-like release sites. Cell 172:706–718.e15.

Liu C, Placais PY, Yamagata N, Pfeiffer BD, Aso Y, Friedrich AB, Siwanowicz I, Rubin GM, Preat T, Tanimoto H (2012) A subset of dopamine neurons signals reward for odour memory in *Drosophila*. Nature 488:512–516.

Lonart G, Cassels KL, Johnson KM (1993) Nitric oxide induces calcium-dependent [^{3}H]dopamine release from striatal slices. J Neurosci Res 35:192–198.

Lu YF, Hawkins RD (2002) Ryanodine receptors contribute to cGMP-induced late-phase LTP and CREB phosphorylation in the hippocampus. J Neurophysiol 88:1270–1278.

Mao Z, Davis RL (2009) Eight different types of dopaminergic neurons innervate the *Drosophila* mushroom body neuropil: anatomical and physiological heterogeneity. Front Neural Circuits 3:5.

Mao Z, Roman G, Zong L, Davis RL (2004) Pharmacogenetic rescue in time and space of the rutabaga memory impairment by using Gene-Switch. Proc Natl Acad Sci USA 101:198–203.

Marin EC, Jefferis GS, Komiyama T, Zhu H, Luo L (2002) Representation of the glomerular olfactory map in the *Drosophila* brain. Cell 109:243–255.

Maruyama T, Kanaji T, Nakade S, Kanno T, Mikoshiba K (1997) 2APB, 2-aminoethoxydiphenyl borate, a membrane-penetrable modulator of Ins (1,4,5)P3-induced Ca^{2+} release. J Biochem 122:498–505.

Matsuda W, Furuta T, Nakamura KC, Hioki H, Fujiyama F, Arai R, Kaneko T (2009) Single nigrostriatal dopaminergic neurons form widely spread and highly dense axonal arborizations in the neostriatum. J Neurosci 29:444–453.

McGuire SE, Le PT, Davis RL (2001) The role of *Drosophila* mushroom body signaling in olfactory memory. Science 293:1330–1333.

McGuire SE, Le PT, Osborn AJ, Matsumoto K, Davis RL (2003) Spatiotemporal rescue of memory dysfunction in *Drosophila*. Science 302:1765–1768.

Meinrenken CJ, Borst JG, Sakmann B (2003) Local routes revisited: the space and time dependence of the Ca^{2+} signal for phasic transmitter release at the rat calyx of Held. J Physiol 547:665–689.

Michel BW, Lippert AR, Chang CJ (2012) A reaction-based fluorescent probe for selective imaging of carbon monoxide in living cells using a palladium-mediated carbonylation. J Am Chem Soc 134:15668–15671.

Miesenbock G, De Angelis DA, Rothman JE (1998) Visualizing secretion and synaptic transmission with pH-sensitive green fluorescent proteins. Nature 394:192–195.

Miyashita T, Oda Y, Horiuchi J, Yin JC, Morimoto T, Saitoe M (2012) Mg (2+) block of *Drosophila* NMDA receptors is required for long-term memory formation and CREB-dependent gene expression. Neuron 74:887–898.

Molina-Luna K, Pekanovic A, Rohrich S, Hertler B, Schubring-Giese M, Rioult-Pedotti MS, Luft AR (2009) Dopamine in motor cortex is necessary for skill learning and synaptic plasticity. PLoS One 4:e7082.

Muller U (1994) Ca^{2+}/calmodulin-dependent nitric oxide synthase in Apis mellifera and *Drosophila melanogaster*. Eur J Neurosci 6:1362–1370.

Muller U (1996) Inhibition of nitric oxide synthase impairs a distinct form of long-term memory in the honeybee, *Apis mellifera*. Neuron 16:541–549.

Ng M, Roorda RD, Lima SQ, Zemelman BV, Morcillo P, Miesenbock G (2002) Transmission of olfactory information between three populations of neurons in the antennal lobe of the fly. Neuron 36:463–474.

Ohata J, Bruemmer KJ, Chang CJ (2019) Activity-based sensing methods for monitoring the reactive carbon species carbon monoxide and formaldehyde in Living Systems. Acc Chem Res 52:2841–2848.

Oyamada T, Hayashi T, Kagaya A, Yokota N, Yamawaki S (1998) Effect of dantrolene on K(+)- and caffeine-induced dopamine release in rat striatum assessed by in vivo microdialysis. Neurochem Int 32:171–176.

Pereira DB, Schmitz Y, Meszaros J, Merchant P, Hu G, Li S, Henke A, Lizardi-Ortiz JE, Karpowicz RJ Jr, Morgenstern TJ, Sonders MS, Kanter E, Rodriguez PC, Mosharov EV, Sames D, Sulzer D (2016) Fluorescent

false neurotransmitter reveals functionally silent dopamine vesicle clusters in the striatum. Nat Neurosci 19:578–586.
Pfeiffer BD, Truman JW, Rubin GM (2012) Using translational enhancers to increase transgene expression in *Drosophila*. Proc Natl Acad Sci USA 109:6626–6631.
Poss KD, Thomas MJ, Ebralidze AK, O'Dell TJ, Tonegawa S (1995) Hippocampal long-term potentiation is normal in heme oxygenase-2 mutant mice. Neuron 15:867–873.
Puig MV, Antzoulatos EG, Miller EK (2014) Prefrontal dopamine in associative learning and memory. Neuroscience 282:217–229.
Regehr WG, Carey MR, Best AR (2009) Activity-dependent regulation of synapses by retrograde messengers. Neuron 63:154–170.
Regulski M, Tully T (1995) Molecular and biochemical characterization of dNOS: a *Drosophila* Ca^{2+}/calmodulin-dependent nitric oxide synthase. Proc Natl Acad Sci USA 92:9072–9076.
Rice ME, Cragg SJ (2008) Dopamine spillover after quantal release: rethinking dopamine transmission in the nigrostriatal pathway. Brain Res Rev 58:303–313.
Rorig B, Klausa G, Sutor B (1996) Intracellular acidification reduced gap junction coupling between immature rat neocortical pyramidal neurones. J Physiol 490:31–49.
Sabatini BL, Regehr WG (1996) Timing of neurotransmission at fast synapses in the mammalian brain. Nature 384:170–172.
Sagara Y, Inesi G (1991) Inhibition of the sarcoplasmic reticulum Ca^{2+} transport ATPase by thapsigargin at subnanomolar concentrations. J Biol Chem 266:13503–13506.
Shibuki K, Kimura S, Wakatsuki H (2001) Suppression of the induction of long-term depression by carbon monoxide in rat cerebellar slices. Eur J Neurosci 13:609–616.
Sinakevitch I, Grau Y, Strausfeld NJ, Birman S (2010) Dynamics of glutamatergic signaling in the mushroom body of young adult *Drosophila*. Neural Dev 5:10.
Stewart BA, Atwood HL, Renger JJ, Wang J, Wu CF (1994) Improved stability of *Drosophila* larval neuromuscular preparations in haemolymph-like physiological solutions. J Comp Physiol A Neuroethol Sens Neural Behav Physiol 175:179–191.
Stone JR, Marletta MA (1994) Soluble guanylate cyclase from bovine lung: activation with nitric oxide and carbon monoxide and spectral characterization of the ferrous and ferric states. Biochemistry 33:5636–5640.
Su H, O'Dowd DK (2003) Fast synaptic currents in *Drosophila* mushroom body Kenyon cells are mediated by alpha-bungarotoxin-sensitive nicotinic acetylcholine receptors and picrotoxin-sensitive GABA receptors. J Neurosci 23:9246–9253.
Sugimura Y, Yoshizaki F, Katagiri J, Horiuchi C (1980) Studies on algal cytochromes: I. Purification and properties of cytochrome b-561 from *Enteromorpha prolifera*. J Biochem 87:541–547.
Sun F, Zeng J, Jing M, Zhou J, Feng J, Owen SF, Luo Y, Li F, Wang H, Yamaguchi T, Yong Z, Gao Y, Peng W, Wang L, Zhang S, Du J, Lin D, Xu M, Kreitzer AC, Cui G, et al. (2018) A genetically encoded fluorescent sensor enables rapid and specific detection of dopamine in flies, fish, and mice. Cell 174:481–496.e419.
Takasago T, Imagawa T, Furukawa K, Ogurusu T, Shigekawa M (1991) Regulation of the cardiac ryanodine receptor by protein kinase-dependent phosphorylation. J Biochem 109:163–170.
Takemura S, Aso Y, Hige T, Wong A, Lu Z, Xu CS, Rivlin PK, Hess H, Zhao T, Parag T, Berg S, Huang G, Katz W, Olbris DJ, Plaza S, Umayam L, Aniceto R, Chang LA, Lauchie S, Ogundeyi O, et al. (2017) A connectome of a learning and memory center in the adult *Drosophila* brain. Elife 6:e26975.
Tamura T, Chiang AS, Ito N, Liu HP, Horiuchi J, Tully T, Saitoe M (2003) Aging specifically impairs amnesiac-dependent memory in *Drosophila*. Neuron 40:1003–1011.
Taskiran D, Kutay FZ, Pogun S (2003) Effect of carbon monoxide on dopamine and glutamate uptake and cGMP levels in rat brain. Neuropsychopharmacology 28:1176–1181.
Tinajero-Trejo M, Denby KJ, Sedelnikova SE, Hassoubah SA, Mann BE, Poole RK (2014) Carbon monoxide-releasing molecule-3 (CORM-3; Ru(CO)3Cl(glycinate)) as a tool to study the concerted effects of carbon monoxide and nitric oxide on bacterial flavohemoglobin Hmp: applications and pitfalls. J Biol Chem 289:29471–29482.
Tully T, Quinn WG (1985) Classical conditioning and retention in normal and mutant *Drosophila melanogaster*. J Comp Physiol A Neuroethol Sens Neural Behav Physiol 157:263–277.
Ueno K, Naganos S, Hirano Y, Horiuchi J, Saitoe M (2013) Long-term enhancement of synaptic transmission between antennal lobe and mushroom body in cultured *Drosophila* brain. J Physiol 591:287–302.
Ueno K, Suzuki E, Naganos S, Ofusa K, Horiuchi J, Saitoe M (2017) Coincident postsynaptic activity gates presynaptic dopamine release to induce plasticity in *Drosophila* mushroom bodies. Elife 6:e21076.
Verkhratsky A (2005) Physiology and pathophysiology of the calcium store in the endoplasmic reticulum of neurons. Physiol Rev 85:201–279.
Vreman HJ, Ekstrand BC, Stevenson DK (1993) Selection of metalloporphyrin heme oxygenase inhibitors based on potency and photoreactivity. Pediatr Res 33:195–200.
Wan K, Moriya T, Akiyama M, Takeshima H, Shibata S (1999) Involvement of ryanodine receptor type 3 in dopamine release from the striatum: evidence from mutant mice lacking this receptor. Biochem Biophys Res Commun 266:588–592.
Wang R, Wu L (2003) Interaction of selective amino acid residues of K(ca) channels with carbon monoxide. Exp Biol Med (Maywood) 228:474–480.
Wang Y, Wu J, Rowan MJ, Anwyl R (1996) Ryanodine produces a low frequency stimulation-induced NMDA receptor-independent long-term potentiation in the rat dentate gyrus in vitro. J Physiol 495: 755–767.
Wang Y, Mamiya A, Chiang AS, Zhong Y (2008) Imaging of an early memory trace in the *Drosophila* mushroom body. J Neurosci 28:4368–4376.
Wong AM, Wang JW, Axel R (2002) Spatial representation of the glomerular map in the *Drosophila* protocerebrum. Cell 109:229–241.
Xu L, Eu JP, Meissner G, Stamler JS (1998) Activation of the cardiac calcium release channel (ryanodine receptor) by poly-S-nitrosylation. Science 279:234–237.
Yagishita S, Hayashi-Takagi A, Ellis-Davies GC, Urakubo H, Ishii S, Kasai H (2014) A critical time window for dopamine actions on the structural plasticity of dendritic spines. Science 345:1616–1620.
Yamasaki M, Takeuchi T (2017) Locus coeruleus and dopamine-dependent memory consolidation. Neural Plast 2017:1–15.
Yasuyama K, Meinertzhagen IA, Schurmann FW (2002) Synaptic organization of the mushroom body calyx in *Drosophila melanogaster*. J Comp Neurol 445:211–226.
Yu D, Akalal DB, Davis RL (2006) *Drosophila* alpha/beta mushroom body neurons form a branch-specific, long-term cellular memory trace after spaced olfactory conditioning. Neuron 52:845–855.
Zalk R, Lehnart SE, Marks AR (2007) Modulation of the ryanodine receptor and intracellular calcium. Annu Rev Biochem 76:367–385.
Zhao F, Li P, Chen SR, Louis CF, Fruen BR (2001) Dantrolene inhibition of ryanodine receptor Ca^{2+} release channels: molecular mechanism and isoform selectivity. J Biol Chem 276:13810–13816.
Zhu XZ, Luo LG (1992) Effect of nitroprusside (nitric oxide) on endogenous dopamine release from rat striatal slices. J Neurochem 59:932–935.
Zhuo M, Small SA, Kandel ER, Hawkins RD (1993) Nitric oxide and carbon monoxide produce activity-dependent long-term synaptic enhancement in hippocampus. Science 260:1946–1950.
Zorzato F, Scutari E, Tegazzin V, Clementi E, Treves S (1993) Chlorocresol: an activator of ryanodine receptor-mediated Ca^{2+} release. Mol Pharmacol 44:1192–1201.